February 2008

Energy from Heated Asphalt Pavements

Laura A. Rockett
Worcester Polytechnic Institute

Abstract

Channeling the heat from heated asphalt pavements into energy can decrease energy costs in an environmentally friendly manner. By determining ways to increase the thermal properties of the asphalt, more energy can be produced. This project investigated the use of various materials, additives, and testing procedures to obtain the greatest energy output from asphalt pavement samples. Materials tested included limestone, granite, recycled asphalt product (RAP), and quartzite aggregates. Glass, Plexiglas, and acrylic paint were tested as possible top insulating materials. Copper and aluminum powder were tested as a material additive to the pavements. A copper pipe was placed 1" below the pavement surface in all of the samples and two different setups were experimented. Tests were performed either with water being heated in a water bath from the copper pipe, or with water flowing through the copper pipes. It was determined from the multiple test procedures that quartzite aggregates, the more thermally conductive material, are the more advantageous aggregate choice. Furthermore, flowing water through a larger surface area of pipe over a longer length of pavement is the best energy transfer system.

Energy from Heated Asphalt Pavements

Worcester Polytechnic Institute
Transportation Engineering

A Master Qualifying Project Report to be submitted to the faculty of
Worcester Polytechnic Institute in partial fulfillment of the requirements for the
Degree of Bachelor of Science

Submitted by:

Laura Rockett

Submitted to:

Prof. Rajib Mallick

February 25, 2008

TABLE OF CONTENTS

TABLE OF FIGURES

Acknowledgements

The following individuals provided valuable information and assistance necessary for the development of this project:

Dr. Rajib Mallick, Associate Professor, Civil Engineering Department, WPI
Bao-Liang Chen, Graduate Research Assistant, Civil Engineering Department, WPI
Don Pellegrino, Laboratory Manager, Civil Engineering Department, WPI
Dean Daigneault, Laboratory Machinist, Civil Engineering Department, WPI
Ryan Cleverdon, REU (Research Experience for Undergraduates) Student and Project Partner
Gerard Moulzolf, American Engineering Testing, Inc.

Mr. Ron Tardiff, Aggregate Industries

Mr. Jeff Carlstrom. New Ulm Quartzite Quarries

Capstone Design Requirement

The capstone design requirement is fulfilled in the MQP through the design of experiments to evaluate the transfer of heat energy from asphalt pavements. This method enables the use of heat energy from the environment in a safe, non-polluting way. The use of such energy systems can help significantly in the society's quest for renewable clean energy.

Introduction

Rising energy costs and the pollution resulting from production of different materials are becoming more and more of a problem in today's world. It has been established that fossil fuels and greenhouse gases can be quite harmful to our environment. Concern over global warming has led researchers to look towards new methods for energy efficient products that can save money and are environmentally sound. Harnessing solar energy presents itself as the most effective and efficient form of energy. Capturing heat from the sun to produce energy can be seen mostly in solar specific cells, panels, and towers. Although limited, there have been research advancements in absorbing and producing solar energy into common structures involving everyday aspects of life.

Relatively new ventures, such as Road Energy Systems from the Netherlands, have developed methods for heating and cooling of roads and buildings from geothermal energy. Pavements demonstrate the ability to absorb and give off thermal energy from the sun; this can be felt by simply walking on a pavement surface barefoot in the heat of the summer. Theoretically, solar energy from the sun can be captured by the aggregates and the asphalt that make up the pavement, put through a liquid-bearing medium to produce the energy, and used to heat or cool anything from the roadways to a near-by office building. Without such a system, although pavement can capture significant amounts of solar energy, much of the heat escapes into the air.

Maximizing the amount of heat that is absorbed by the pavement is an area where there has been relatively little research. Harnessing as much solar energy as possible would increase the efficiency of the pavements ability to produce energy. Increasing the overall yield of energy from pavement involves increasing the thermal conductivity of the aggregates/and or the mix used in the pavement. This can be done by using different aggregates and/or material additives that would increase the thermal conductivity. Using a thermal insulator on the top layer of the pavement to trap the heat within the pavement would prevent long wave radiation back into the atmosphere.

Producing a energy system for a roadway could prove to be relatively expensive if a large area of road is used. Prices of the pavement would increase with the addition of thermally conductive or top-insulating materials. As roadways are subjected to significant amounts of traffic volumes each day, the wear and tear on the road would require repairs every couple of years. The energy system could be affected each time a repair to the road is made. Considering these factors, parking lots are more ideal than roadways to produce energy because of their relatively small size in comparison with roadways. Parking lots experience much less vehicle traffic each day, making it much easier to construct and maintain a geothermal system within the pavement.

This research was conducted to evaluate the potential of capturing solar energy from asphalt pavements, and to investigate different ways in which the efficiency of such a system can be enhanced. Testing of two different aggregates, quartzite and limestone were conducted to evaluate the effect of aggregate thermal conductivity on heat transfer from heated pavements. A conductivity enhancing additive was mixed with the aggregates which were then mixed with asphalt to produce test samples. These samples were then tested to determine the effectiveness of the additives. Copper powder was chosen as preliminary tests to establish if a metal additive would increase the geothermal energy. Thermally insulating the top layer of the pavement involved testing with a glass cover and acrylic paint. A glass cover was tested with hopes of creating a “greenhouse like” effect with the pavement. Light would enter through the glass but the heat and energy would then be trapped within the pavement sample. The intention of these tests were to lead to preliminary results on what types of aggregates, what kinds of additives, and what types of top insulating materials could be used in the field to create a parking lot with maximum energy yield.

In general, two different testing procedures were used. The first test involved a copper pipe below the surface of the pavement samples. The pipe was put into the sample and heat was allowed to travel along the pipe into a water bath. The change in water temperature was recorded in the water bath for a specific period of time. The second test involved a water pump setup where the copper pipe was put through the entire sample and water was pumped through the pipe while the sample was heated. The temperatures of the incoming and outgoing water were noted to determine the energy produced. Each test was altered based on certain variables to determine the test procedure that produced the largest amount of energy: these changes included using a larger sample area, testing with the various samples, and varying the flow of water through the pipes.

Producing an efficient source of energy that is environmentally safe within a parking lot will prove to be an innovative and useful tool in the world today. The heating and cooling of a near-by building from a parking lot will certainly create an energy source that is inexpensive in a world where energy costs continue to rise.

Background

Heat Transfer

There are three basic mechanisms of heat transfer; conduction, convection, and radiation. The difference in these kinds of heat transfer relate to how the heat is exchanged.

In conduction, heat is transferred by means of molecular agitation within a material without any motion of the material as a whole. For example, if one end of a metal rod is heated the temperature at the other end will rise due to heat conduction. Heat transfer due to convection is from mass motion of a fluid such as air or water when the heated fluid is caused to move away from the source of heat, carrying energy with it, such as boiling water. Heat transfer by convection can also lead to circulation of the fluid.

Radiation is heat transfer by the emission of electromagnetic waves which carry energy away from the emitting object. The greenhouse effect is due to radiation when the short wavelengths of visible light from the sun pass through a transparent medium, such as glass, and are absorbed while the longer wavelengths of the infrared re-radiation from the heated object on the other side of the transparent medium are unable to pass through. The trapping of the long wavelength radiation leads to more heating and a higher resultant temperature. (1)

Also important parameters for heat transfer are thermal conductivity and heat capacity. Thermal conductivity, or k-value, is the ability of a material to conduct heat. Heat capacity is the measure of the heat energy required to increase the temperature of an object by a certain temperature interval. Heat capacity is an extensive property because the value is proportional to the amount of material.

The values provided in the recently released NCHRP mechanistic-empirical

27 design guides (2) were considered. The ranges for asphalt materials are 0.76 to 1.4 W/ (m·K) for thermal conductivity and 921to 1674 J/ (kg·K) for heat capacity.

Geothermal Energy

Geothermal energy is created from the heat of the earth. Typically the heat necessary to develop geothermal energy is drawn from several sources. Hot water or steam reservoirs from drilling, geothermal reservoirs near the earth's surface, or in the shallow ground near the Earth's surface that constantly stays at a temperature of 50°-60°F. The hot water or steam can then be used to drive generators that produce electricity that can be then be used for a variety of applications. (3)

Geothermal energy also has an environmental benefit because it offsets pollution that would have been created if fossil fuels were used as the energy source. (4)

Similar Geothermal Systems

Invisible Heating Systems

In 2006, IHS (Invisible Heating Systems) installed a Road Energy System at the parking lot of their new offices located in the Scottish Highlands. This new system utilizes the heat absorption capacity of asphalt. Their system is capable of heating and cooling buildings or roads and airport runways to keep them free of ice and snow. Using this system is incredibly environmentally beneficial as the CO_2 emissions are lessened by 50-90% compared to traditional heating methods. The Road Energy System is comprised of an asphalt concrete layer with a reinforced structure and a water bearing medium such as pipes. In summer, the Road Energy System generates considerable heat. In the right conditions it is possible to store the heat for the winter and conversely store the cold water for cooling in the summer time. The water is stored in an aquifer under the ground. In addition to the many applications, the system also increases the life of asphalt and reduced the maintenance from thermal damage to the asphalt. (5)

Geothermal HVAC Systems

GeoMax, a geothermal HVAC system provider has developed a system of looped pipes that use geothermal energy to provide air conditioning in the hot weather. Because the pipes are in the ground and the Earth is able to store heat well, the water circulating through the pipes stays hot. About 8 feet below the Earth's surface maintains the same temperature year round. The water is then transferred to a heat pump and then through refrigeration process and then the cool air is blown into buildings as an air-conditioner. The benefits of using this geothermal system are that, along with being environmentally friendly, it is inexpensive to operate and can significantly reduce fuel costs.

Electrically Conductive HMA

A study (6) was conducted to explore the possibility of producing conductive hot mix asphalt mixtures through the use of electrically conductive additives. In the study, the group added micron-scale steel fiber, aluminum chips, and graphite in HMA mixtures to attempt to increase conductivity. For the steel fiber sample, the fibers were blended into the asphalt before being added to the aggregates whereas with the other aluminum and graphite samples, the additives were mixed in with the heated aggregates before mixing. The samples were compacted with the Marshall Hammer. After testing for electrical conductivity, the group concluded that:

- The addition of electrically conductive additives can improve the electrical conductivity of an HMA mixture.
- High aspect-ratio micron scale steel fibers improved the conductivity significantly.
- Even high percentages of aluminum chips failed to improve conductivity appreciably. (6)

Objectives

Problem

With the limited number of sunlight solar cells available, research in finding alternate sources of supplying similar renewable energy are being explored. An asphalt pavement parking lot stores a large amount of heat that could possibly be harvested and used similarly to sunlight solar cells. The heat produced from the pavement may be converted from heat energy into electricity. Figure 1, as seen below, illustrates the concept behind this problem. Since asphalt pavement parking lots exist and are going to continue to exist for a while to come, it only makes sense to try and utilize any additional uses that can be produced from it.

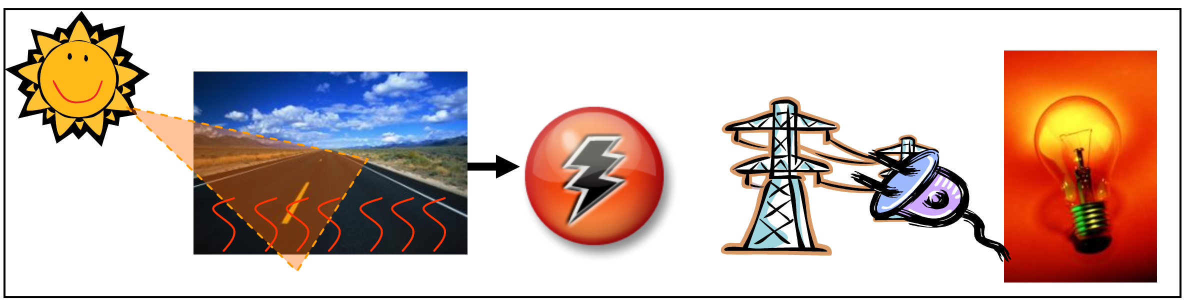

Figure 1: Concept of Project

Objective

The objectives of this study were to: 1. Investigate the effect of thermal conductivities of aggregates, quartzite and limestone, on the amount of energy that can be captured from heated asphalt pavement mix, 2. Determine if additives such as metal powders and coatings such as glass or acrylic paint can increase the efficiency of the heat transfer mechanism, 3. Investigate the option of providing larger surface area of asphalt mix to increase heat transfer, and 4. Evaluate the concept of using water, flowing at an optimum rate, to transfer energy from heated pavements. The heat produced from the samples can be used to create energy through the assistance of generators.

Scope

The first step in this project was to identify two aggregates with different thermal conductivities, or k values. Maximizing these values through use of water and of additives to the asphalt mixtures might increase the amount of heat available to convert into electricity therefore increasing the amount of electricity available from a given pavement.

Since using frequently traveled roads, such as highways and streets would be impractical, using the pavements in parking lots would be optimal. Since parking lots withstand lighter loads, the structural strength of such pavements would be of less concern, and hence these pavements could accommodate a heat transfer system without any major problem.

This project tested the two aggregates, limestone and quartzite, to compare difference in temperature. The quartzite aggregate, because of its very high quartz content, has a much higher k value, than limestone. With the limestone aggregates having a thermal conductivity, k, anywhere between 1.26-1.33 W/m*K, and quartzite aggregates having a k value of 5.38 W/m*K. (7)

The first phase investigated the differences in heat obtained from the two different aggregate mixes. The impact of using water as a heating source was then tested through the copper pipe being placed inside the sample to be heated by the asphalt and aggregates. Next, water was pumped through the sample at different rates to determine positive affects on heating the water, if any. Increasing the surface area of the sample was then tested to determine any difference in the temperature of the water. The final test to increase the thermal conductivity of the pavement was to try various additives either mixed in or on top of the samples which proved to be the most conductive. The additives tested include, glass, Plexiglas, copper, aluminum, and acrylic paint. The Glass, Plexiglas, and acrylic paint were used on the surfaces of the samples tested while the powdered copper and powdered aluminum were mixed with asphalt. After this testing was completed, the optimal aggregate and later the most promising additives were used in a large-scale sample tested outside under true conditions with water flow.

Mix Designs Procedure:

For each batch, PG 64-28 asphalt was used at 5.5% asphalt content. Mixing was conducted at 150C and compaction was completed at 140-145C. Following standard HMA mixing and compaction procedures, the mix was aged for two hours and the samples were compacted to 75 gyrations. After the samples were allowed to cool the bulk specific gravities were determined using the CoreLok method. This method allows testing without exposing the samples to water.

With the exception of the samples that were mixed with the material additives, the mix design procedure remained the same whenever a sample was produced. The copper powder was added to the mix design to create a mix that was 22% copper. The mix design for the copper powder sample added 997.5 g of copper powder and 305.25 g of PG64-28 asphalt. The sample was aged for two hours, compacted to 75 gyrations, allowed to cool, and was then prepared for testing.

Of the small samples, eight were produced for testing: one limestone sample, one quartzite samples, one quartzite-copper sample, one quartzite-aluminum sample, one RAP sample, 2 combination quartzite/RAP samples and one Wrentham (granite) sample. The quartzite samples with copper and aluminum were used for the testing of top insulating materials. All of the samples had 150 mm diameters with heights of 117 mm. The samples were reused for numerous tests if they were not disturbed or broken in any way.

For the construction of the slab samples, much greater volumes of aggregate were needed. A 3’x6’mold was assembled on wheels to easily move the slab in and out of the laboratory. Two slabs were constructed; one of 100% granite aggregate from Wrentham and the second of 25% granite on the bottom layers and the other 75% of quartzite aggregate from Sioux Falls, IN. The slabs were constructed in approximately 5 lifts, each of about 1” of aggregate in the slab being compacted at each lift. At certain lifts, thermocouples were placed inside of the slab sample for future testing. Before the last lift on each sample, a copper frame was placed to be located approximately one inch from the surface of each. After some testing of the slabs, an acrylic paint topcoat was placed on 1/3 of the surface of Wrentham slabs surface to test for increased conductivity.

Procedure:

Tests Setup Procedure:

Thermocouples

Thermocouples were used for the various testing procedures all samples to collect temperature data. Each thermocouple was used to give a minute by minute reading of the temperature of the location where it was placed. The temperature readings were shown in a spreadsheet each minute they were produced, and they were also graphed on a temperature versus time plot. The collected data was then analyzed based on temperature changes in the water baths, pavement layers or the air. Figure 2 shows the thermocouples connected to the National Instruments SC-2345 Signal Conditioning Connector Block. The SCC block is then connected to the computer where the temperature readings were given.

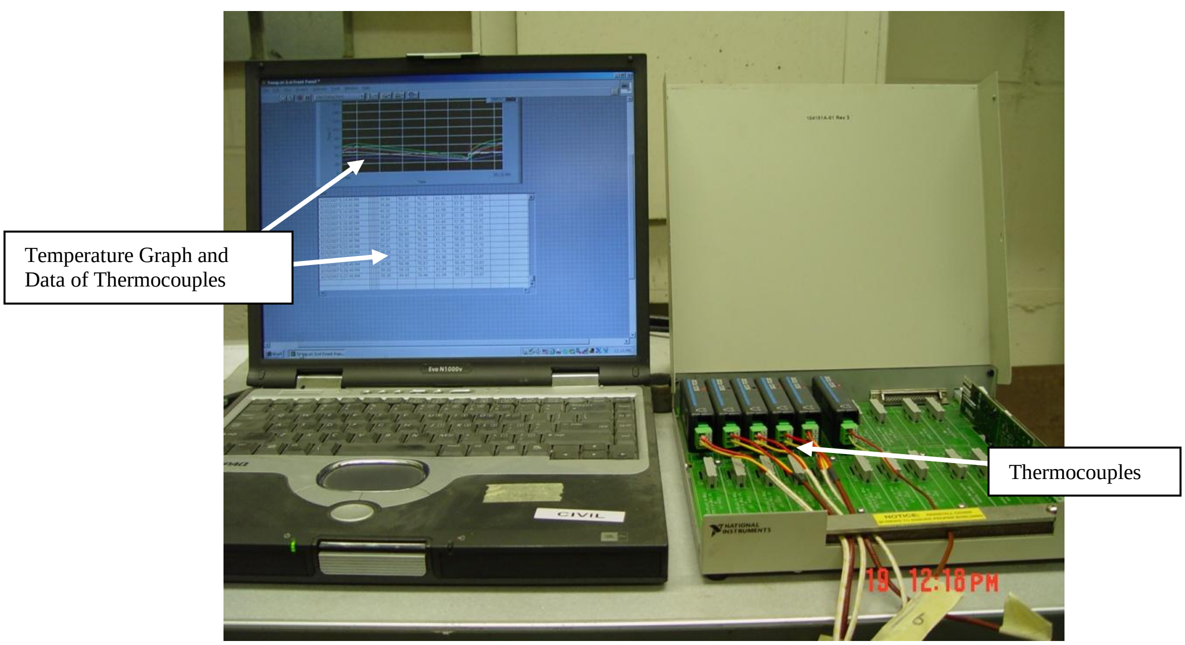

Figure 2: Thermocouple Setup

The same system of retrieving thermocouple data was used for the slab testing as well with similar spacing of thermocouples within the sample. Figure 3 shows the placement of a thermocouple on the surface of a sample.

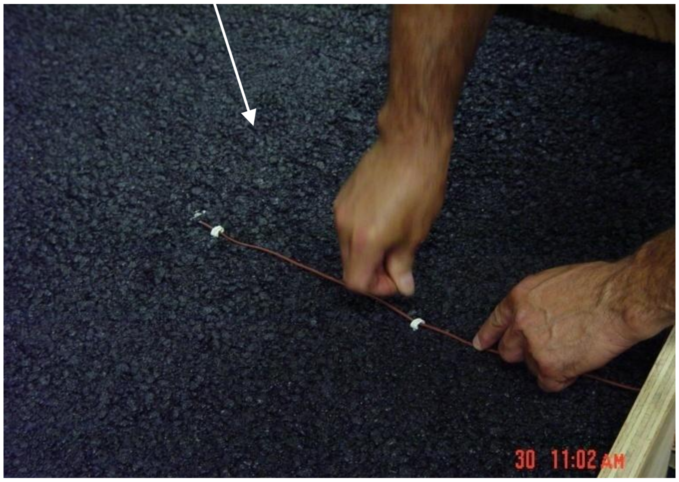

Figure 3: Thermocouple in Slab

Copper Pipe in Water Bath Setup

The initial test procedure involved drilling a ½” hole into the pavement sample 25.4 mm (1”) below the surface. This hole was not drilled completely through the sample, but as far in as possible without disturbing the sample. Three small ¼” holes were drilled on the opposite side, 25.4 mm below the surface, the middle of the sample (55 mm below surface), and 91.6 mm below the surface (1” from the bottom). These holes were for the locations of the thermocouples for measuring the temperature changes in the pavement. The ½” copper pipe was inserted into the pavement sample, the pipe was then run through a ½” hole in the 150mm x 150 mm x 75 mm water bath. Figure 4 shows the schematic diagram of the water bath setup, the locations of the thermocouples in the water bath and the pavement sample are shown and labeled according to how they were plotted on the computer. The density of the sample, either quartzite or limestone, is shown within the sample.

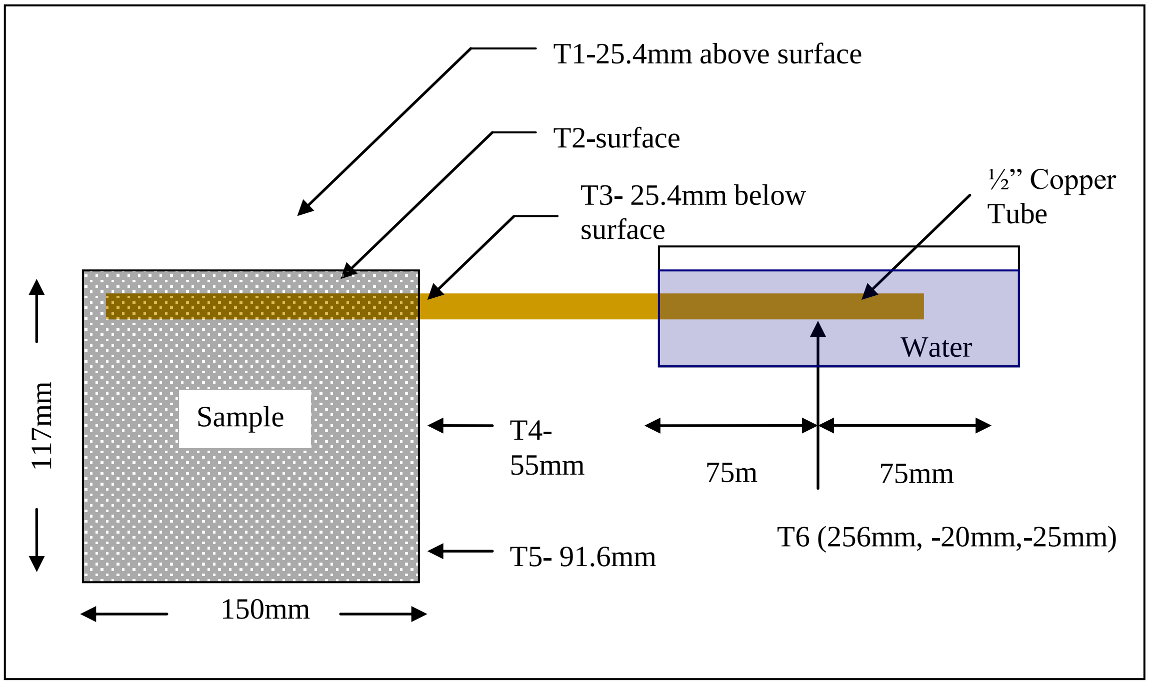

Figure 4: Copper Pipe in Water Bath Setup

Figure 5 shows a picture of the copper pipe in water bath setup. The ½” copper pipe was fabricated so that there was enough room for the pipe to go from the end of the pavement sample into the water bath without the partition wall creating a problem. This wooden partition wall was created to block the heat from the halogen lamp from disturbing the thermally insulated water bath. The pavement sample, the copper pipe, and the water bath were insulated completely to decrease the amount of heat escaping into the air.

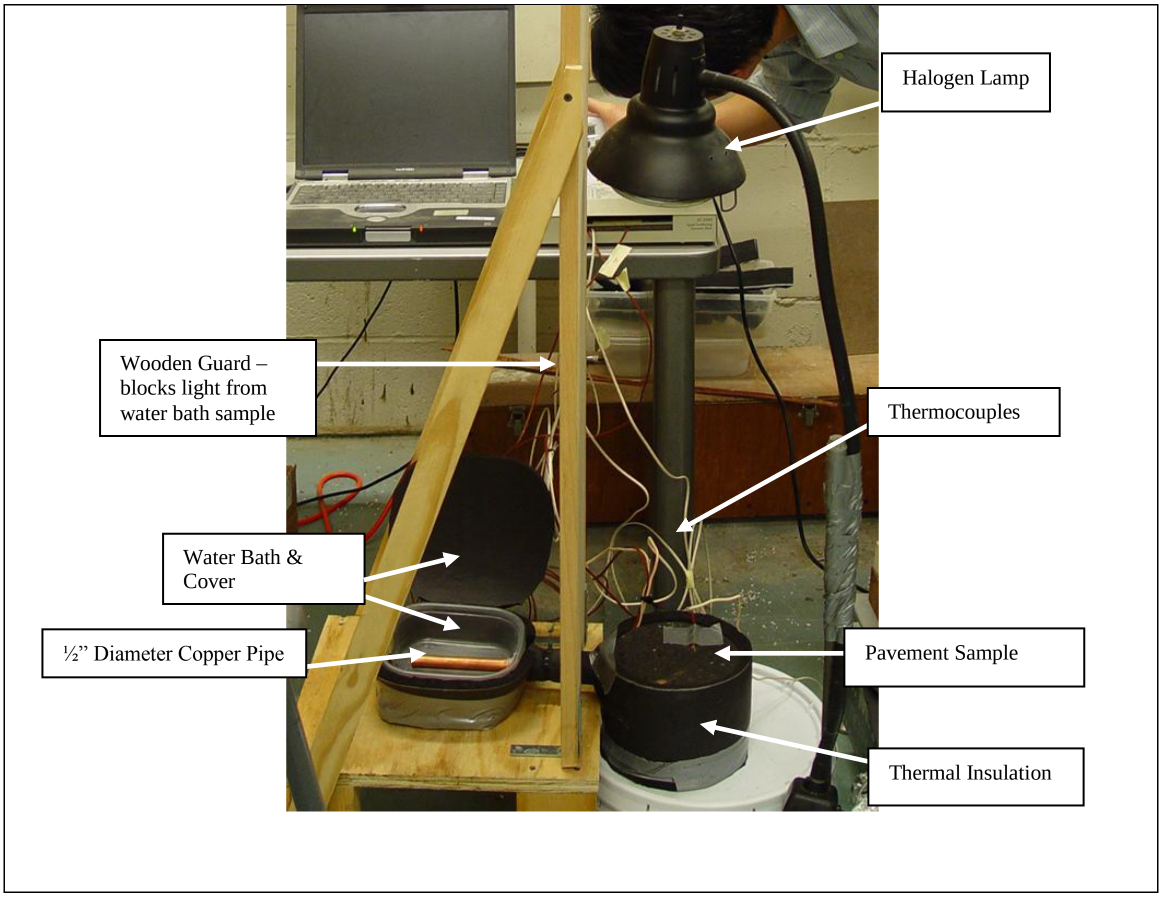

Figure 5: Copper Pipe in Water Bath Setup

The sample was heated for six hours by the 100 Watt halogen lamp which was positioned to be 52 cm above the surface of the pavement. At this height, the light on the surface of the pavement sample was 1000 W/m^2, which is the approximate solar radiation in Worcester. All tests that were performed had the halogen lamps positioned so that the light was 52 cm from the surface of the pavement. Each thermocouple gave a temperature reading each minute that could be read directly from the computer. From the change in temperature of the water bath over the six hour period the amount of energy was calculated using the $Q=m*c*\Delta t$ equation. Where m is the mass of the water bath in ml, c is the specific heat of water (4.187 J/g), and Δt is the change in temperature of the water bath over the six hour period. This test procedure was performed on four different samples: a limestone sample, a quartzite sample, a quartzite sample with Plexiglas, and a quartzite sample with glass. The same quartzite sample was used for each of the tests with the Plexiglas and the glass.

Water Pump Setup

The water pump setup involved drilling a ¼" hole completely through a quartzite sample 25.4 mm below the surface of the pavement. A ¼" diameter copper pipe was inserted through the hole so that it fit snuggly into the sample. Two small ¼" diameter holes were then drilled 25.4 mm below the surface, and 91.6 mm below the surface (1" from the bottom) to fit the thermocouples. Figure 5 displays a schematic of the water pump set up, in which water was pumped through the copper pipe into a water bath where the outlet water flow temperature was taken. The thermocouples are labeled corresponding to their number in the SCC block and on the computer.

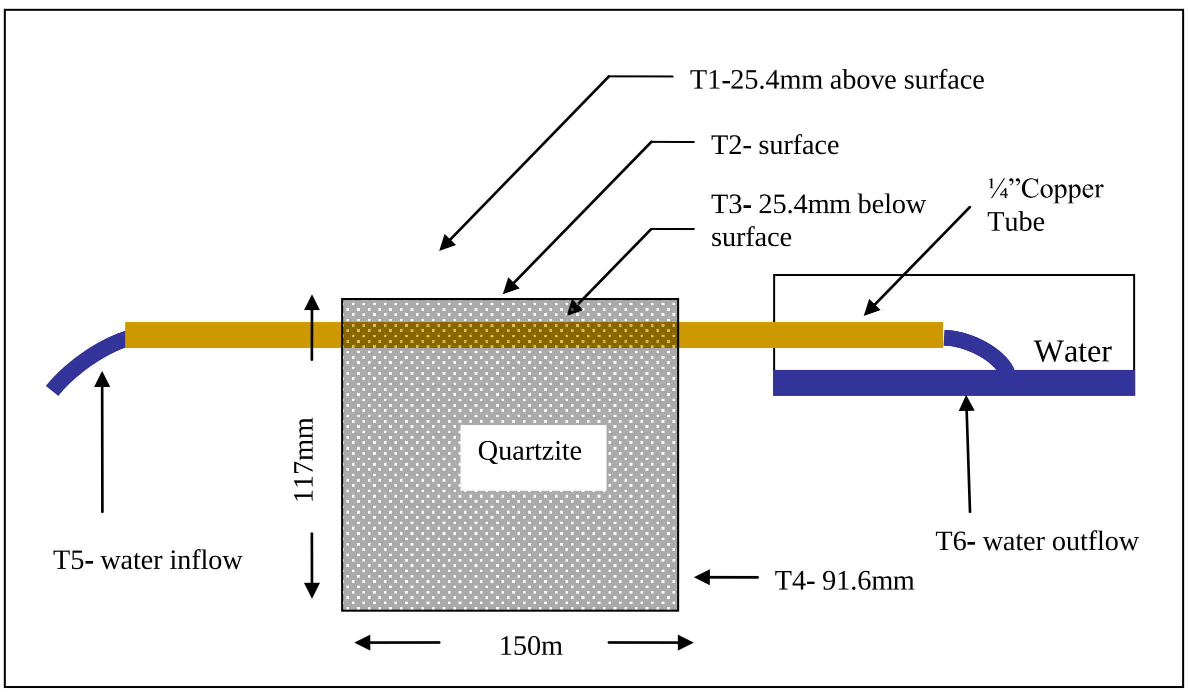

Figure 6: Water Pump Setup

The water pump used allowed for flow rates anywhere between 1ml/min to 100 ml/min to be pumped through the ¼" copper pipe. One end of the plastic pump tubing was put into a large water bucket with a thermocouple. The bucket was covered to keep the temperature of the water from being disturbed. The outlet flow of the pump connected the rubber tubing to the ¼" copper pipe. The water was put through the sample under a 100 watt Halogen lamp that heated the sample. The halogen lamp was turned on 6 hours prior to starting the experiment so the pavement and the copper pipe was heated before the experiment was performed. The outlet of the pipe emptied the water into a small insulated water bath where a thermocouple took the temperature reading of the heated water. A small valve emptied the excess water in the water bath into a large outlet bucket; this allowed for new water to circulate and fill up the water bath every couple of minutes. Figure 6 shows a picture of the water pump setup. As with the copper tube into the water bath setup, the copper pipe, pavement sample, and water bath were thermally insulated to trap any escaping heat during the testing process.

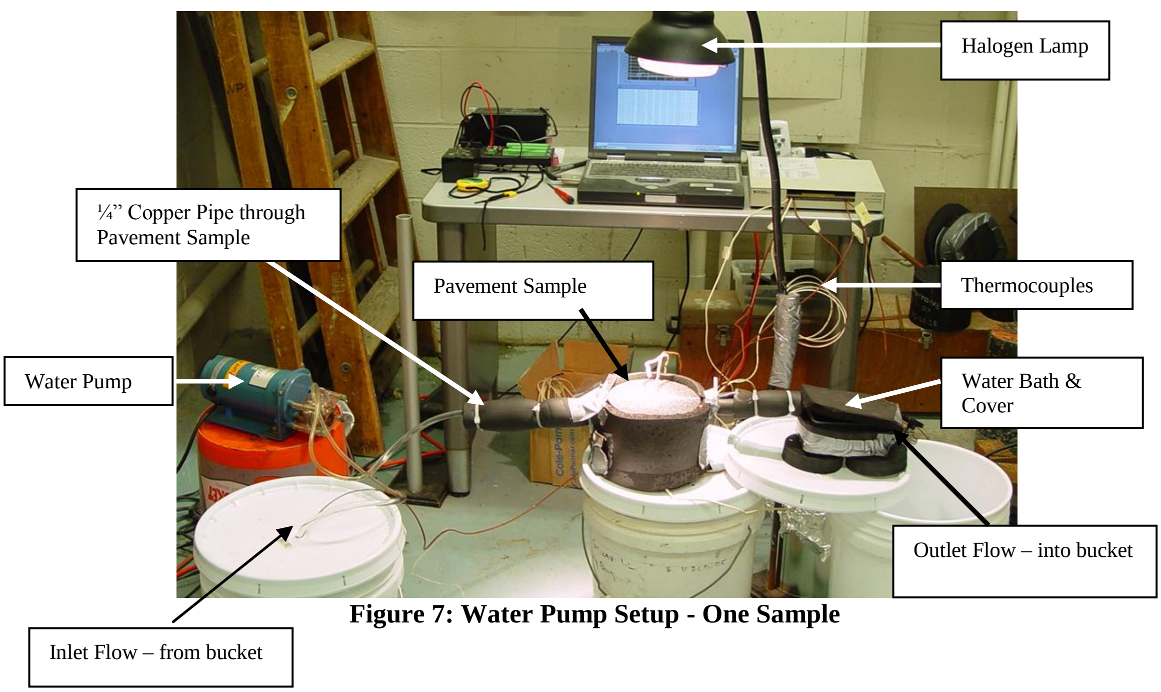

Figure 7: Water Pump Setup - One Sample

Water was pumped through the pavement sample via the copper pipe at varying flow rates until a constant temperate was noted at the outlet where the water bath was located. The constant temperature indicated that equilibrium had been established at the current flow rate. The following flow rates were pumped through the sample: 1 ml/min, 3 ml/min, 5 ml/min, 8 ml/min, 10 ml/min, 20 ml/min, 30 ml/min, 40 ml/min, 50 ml/min, 60 ml/min, 70 ml/min, 80 ml/min, 90 ml/min, and 100 ml/min. The 3 ml/min flow was performed using ice water in the outlet bucket to determine if the initial temperature of the water had any effect on the energy and power produced. There was no specific duration for each flow, if a constant temperature was noted than the flow rate was increased and the same procedure was performed. Varying the flow rates indicated if there was any correlation between the amount of energy produced and how quickly the water was flowing through the pipe.

The power generated for each flow rate was calculated based on calculating the heat flux per unit area, which was calculated from the following equation:

$$q = h * \Delta t$$

Where q is the heat flux per unit area in W/m^2, h is the heat transfer coefficient in W/m^2, and Δt is the change in temperature from the water bucket to the water bath. Multiplying the heat flux per unit area by the cross sectional area of the copper pipe gave the power generated (W), in Watts, for the corresponding flow rate. The energy (Q), in joules, was then calculated by multiplying the power by the duration of the flow (seconds).

The copper powder sample was performed using the same procedure so that comparisons could then be made to determine if the material addictive would increase the power and energy produced from the asphalt pavement sample.

Standing Water Setup

A test was then performed using the same setup with the exception that the outlet of the ¼" copper pipe was standing with duct tape so that the water was held in the pipe for a designated period of time. The water in the pipe was then pumped out and the temperature of the water was determined using a thermocouple in the small water bath where the water was emptied.

To determine the amount of water that was held in the copper pipes the pump was used to clear all water out of the tubes, water was then pumped slowly into the pipe until it began to flow out the outlet. The time for the water to travel from one end of the pipe to the other was the amount of time it took for all the water to be pumped out into the water bath. This gave a fairly accurate temperature reading of only the water that had been standing in the pipe, and not any of the water in the tubing.

The water was held in the pipe with the 100 watt Halogen lamp still heating up the sample. This was done for increments of 5 minutes, until the standing water was held in the copper pipe for 30 minutes. The initial and final temperatures were recorded to determine the temperature change of the water as the duration increased.

22% Copper Additive Sample

A sample was constructed using quartzite aggregates, substituting some of the fine aggregates for a powdered copper additive. The addition of powdered copper was to increase the thermal properties of the sample with the use of the most thermally conductive aggregate. The samples was set up similar to the single quartzite sample, with a ¾" copper pipe placed 1" below the surface of the sample and with water pumped through that pipe at various flow rates. Figure 10, below, displays a schematic of the copper samples. Similar to the other samples, the copper sample was pre-heated for six hours in advance. The same calculations were then figured when the testing was completed to determine if the addition of copper to the quartzite enhance the samples ability to produce power.

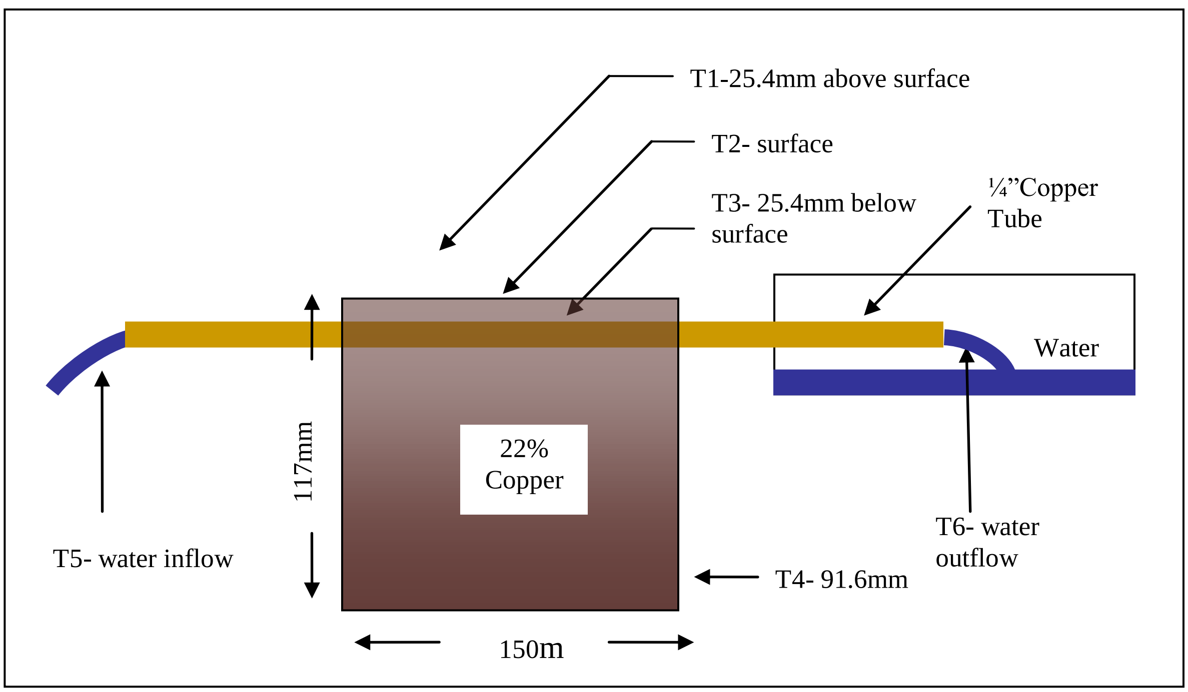

Figure 8: Copper Powder Sample

Slab Testing

After the slabs were constructed, complete with thermocouples permanently in-place, the slab to be tested was transported outside of Kaven Hall. Each of the four copper

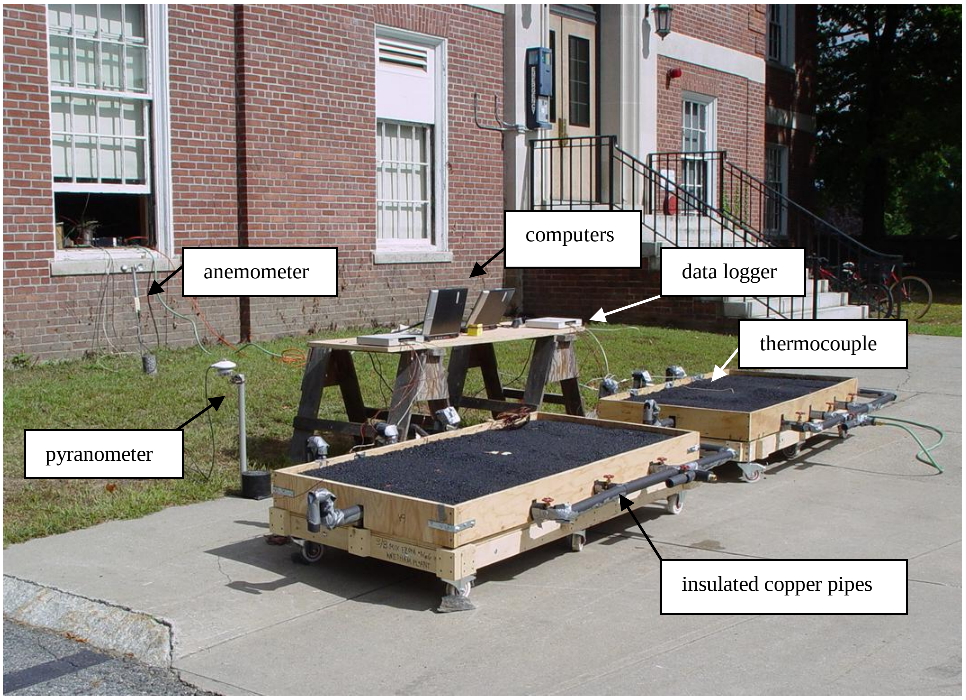

Figure 9: Both Slabs Outside During Testing

pipes in the frame were constructed with a stop valve so that different areas could be tested at different times. Once the slab was in place outside, the computer was brought outside to connect to the thermocouples to read the temperatures. A thermometer was placed outside and hourly readings were recorded to track the ambient temperature. Additionally an anemometer, used to measure wind, and a pyranometer, used to measure solar radiation, were both placed outside by the slab during testing.

Figure 11: Anemometer

Figure 10: Pyranometer

Several tests were run with both samples with water being pumped through various piped in the sample and at flow rates varying from 300mL-4L/min. Testing was conducted on relatively sunny days in the Fall with recorded ambient temperatures around 30-40C.

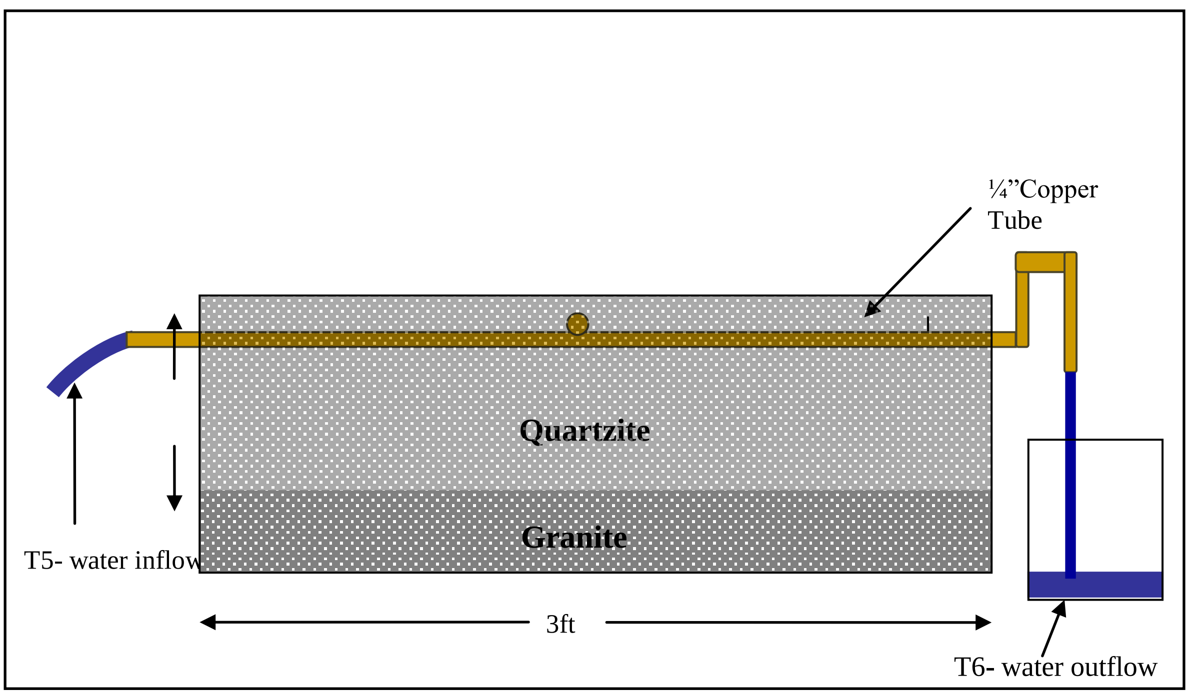

Figure 12: Slab Setup

Sample Case Directory:

Case 1: Quartzite

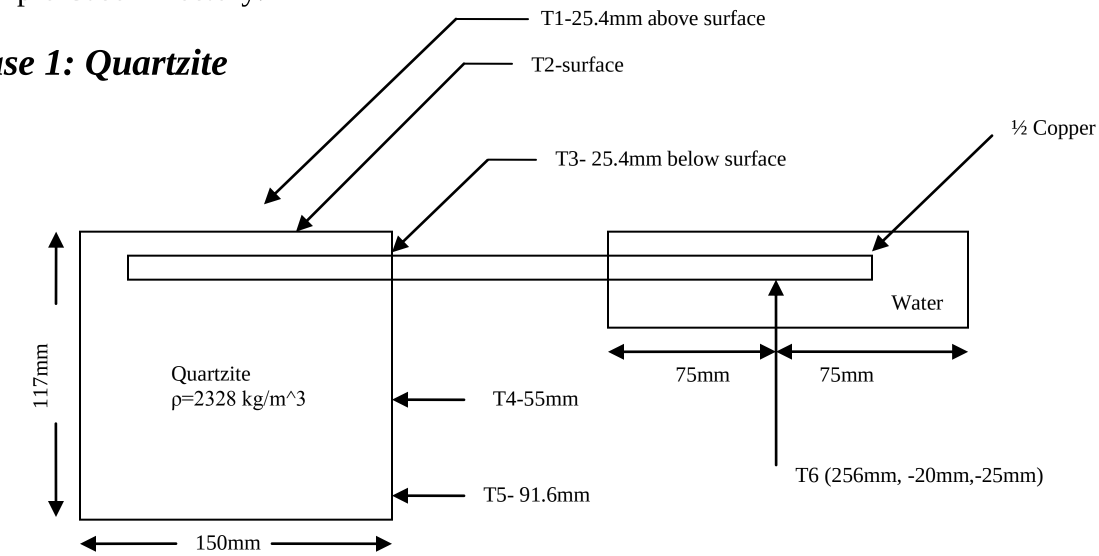

Figure 13: Schematic of 6" Quartzite Sample

The sample labeled Case 1 is a sample made entirely with quartzite aggregates. A ½” copper pipe was placed one inch below the surface of the sample and was connected to a water bath to measure the thermal increase of the copper pipe from the sample. Thermocouples (labeled as T1-T6) were placed strategically to collect optimal data in sample layers as well as in the water.

Case 2: Limestone

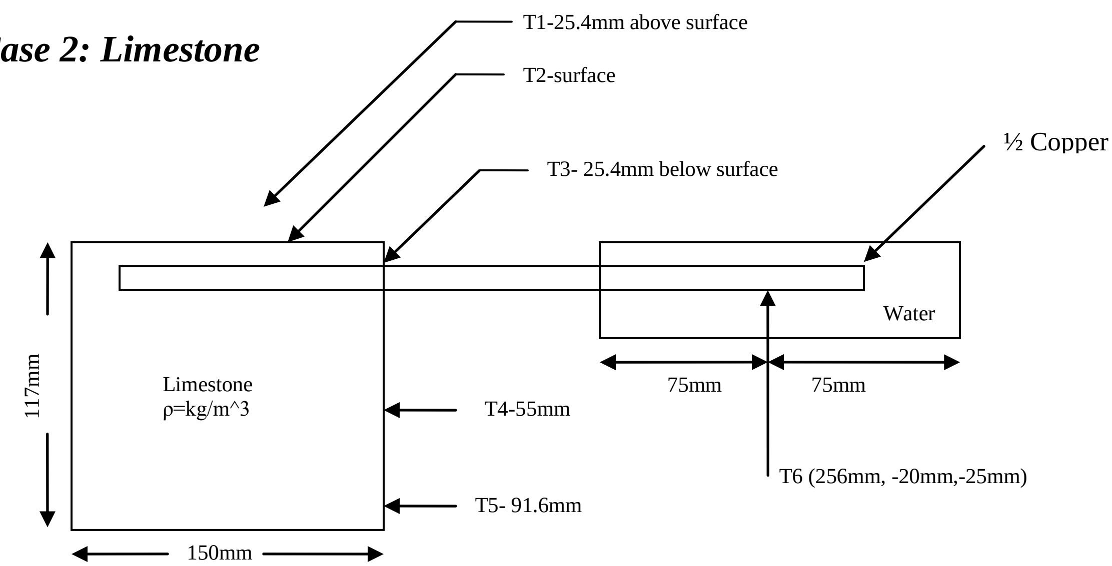

Figure 14: Schematic of Limestone 6” Sample

The sample labeled Case 2 is a sample made entirely with limestone aggregate. ½” A copper pipe was placed one inch below the surface of the sample and was connected to a water bath to measure the thermal increase of the copper pipe from the sample. Thermocouples (labeled as T1-T6) were placed strategically to collect optimal data in sample layers as well as in the water.

Case 3: Quartzite with Glass Disc

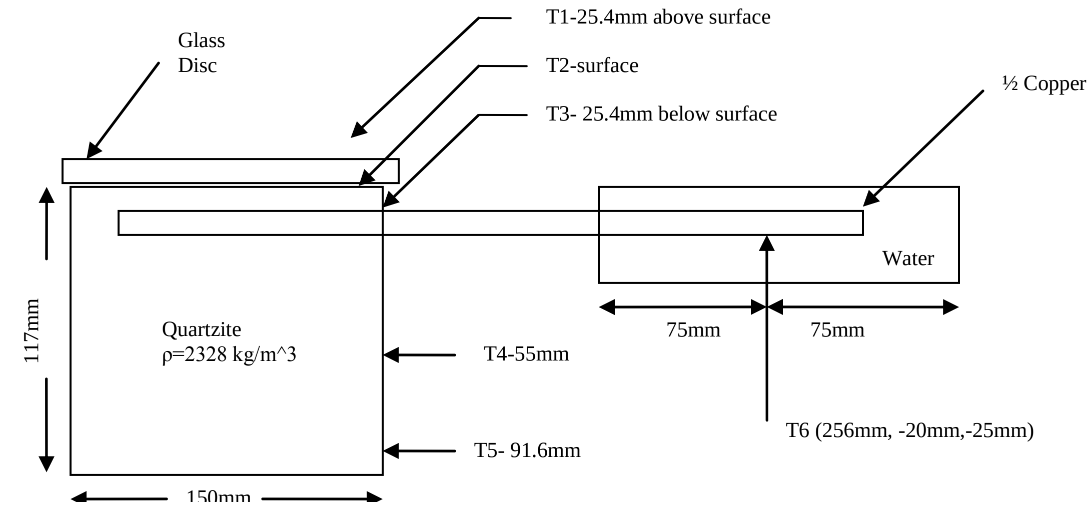

Figure 15: Schematic of Quartzite w/ Glass Disc

The sample labeled Case 3 is a sample made entirely with quartzite aggregates. The sample was tested with a glazed glass disc placed over the sample. A ½" copper pipe was placed one inch below the surface of the sample and was connected to a water bath to measure the thermal increase of the copper pipe from the sample. Thermocouples (labeled as T1-T6) were placed strategically to collect optimal data in sample layers as well as in the water.

Case 4: Quartzite: Ice-Water w/ 3mL Flow and Steady Water

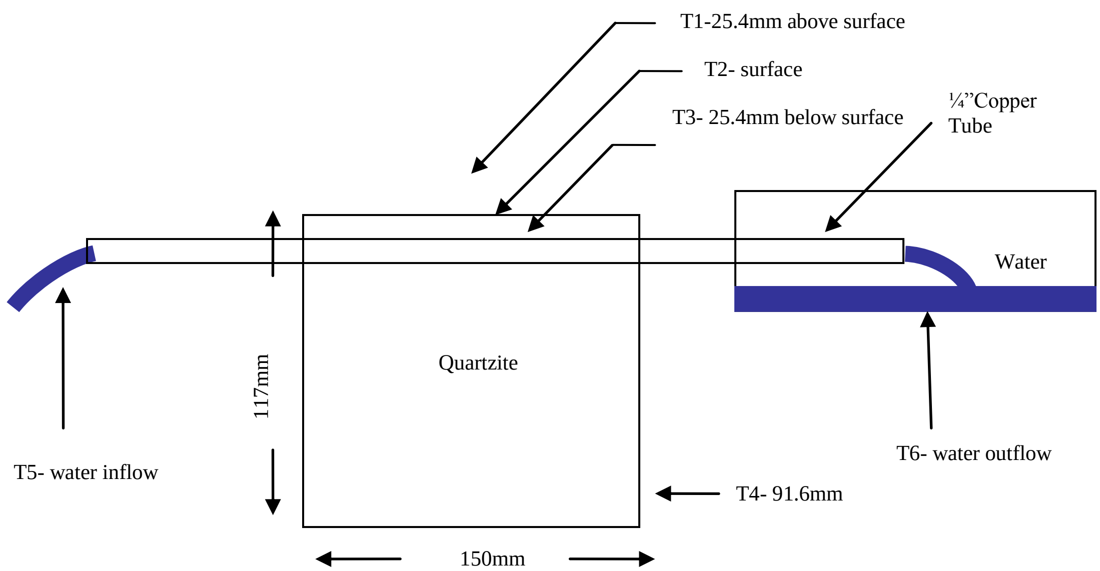

Figure 16: Schematic of Ice-Water w/ 3mL Flow and Steady Water

The sample labeled Case 4 is a sample made entirely with quartzite aggregate with a ¼" copper pipe that had ice-water pumped at a steady flow rate of 3mL/minute. Thermocouples (labeled as T1-T6) were placed strategically to collect optimal data in sample layers as well as in the water.

Case 5: Ice-Water w/ 3mL Flow and Steady Water

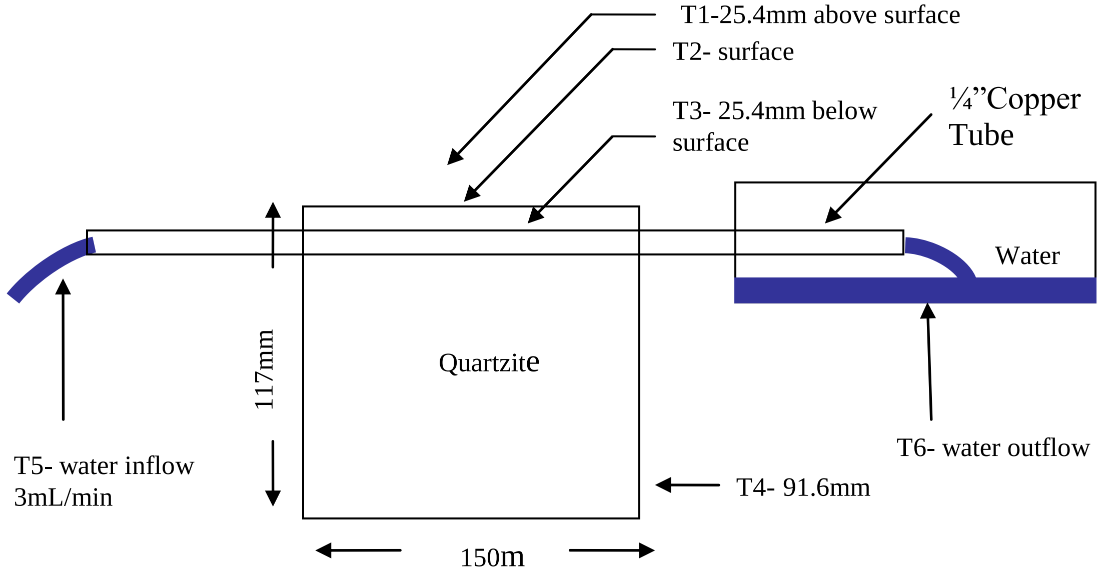

Figure 17: Schematic of Ice-Water w/ 3mL Flow and Steady Water

The sample labeled Case 5, similar to case 4, is a sample made entirely with quartzite aggregate with a ¼" copper pipe that had ice-water pumped at a steady flow rate of 3mL/minute.

Case 6: HMA Compiled w/ Water Flow

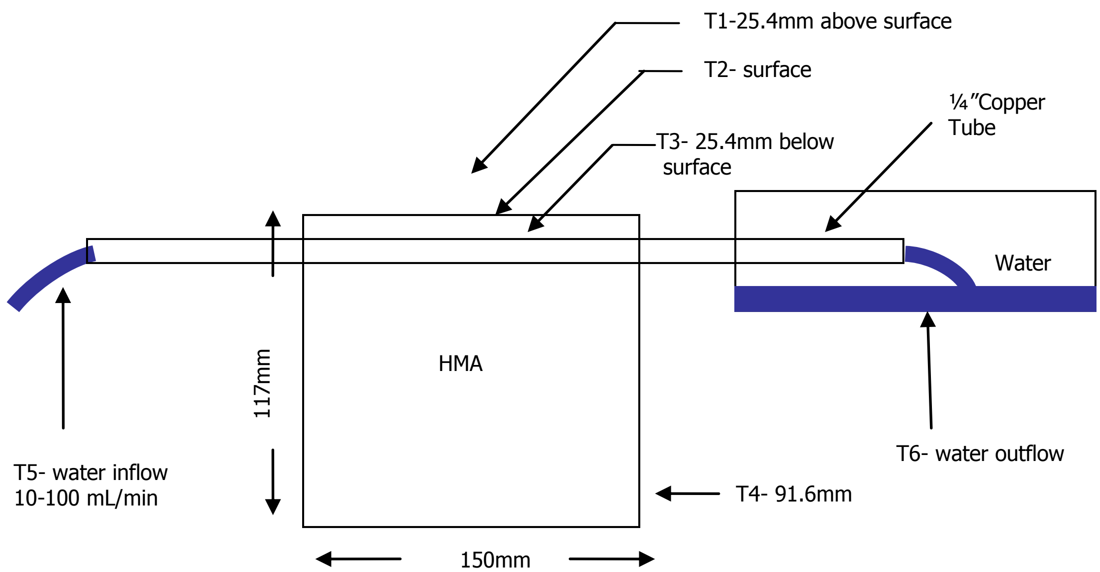

Figure 18: Schematic of HMA w/ Water Flow

The sample labeled Case 6, is a sample made entirely with quartzite aggregate with a ¼" copper pipe in the sample 1" below the surface. The system had ice-water pumped at a flow rate of 10mL/min originally and was tested in the same system increasing by 10nL/min up to 100mL/min.

Case 7: Quartzite w/ 22% Copper

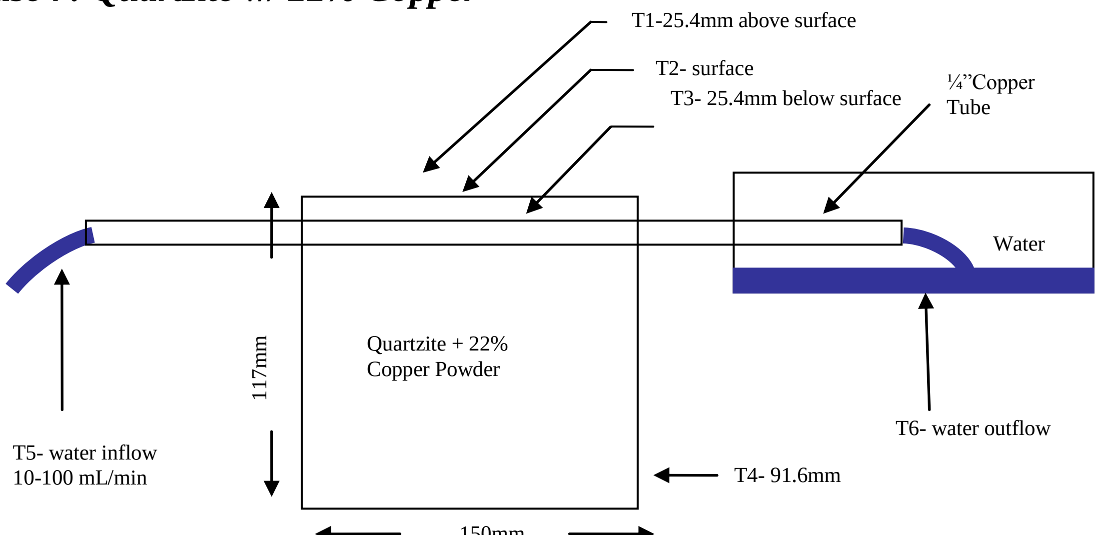

Figure 19: Schematic of Quartzite w/ 22% Copper

The sample labeled Case 7 is a sample made with quartzite aggregate enhanced with 22% copper powder with a ¼" copper pipe in the sample 1" below the surface. The system had ice-water pumped at a flow rate 1mL/min, then 5mL/min, similarly at 8, 10, 20, 30, 40, 50, 60, 70, 80, 90, and 100mL/min.

Case 8: Quartzite w/ 22% Copper and Glazed Glass

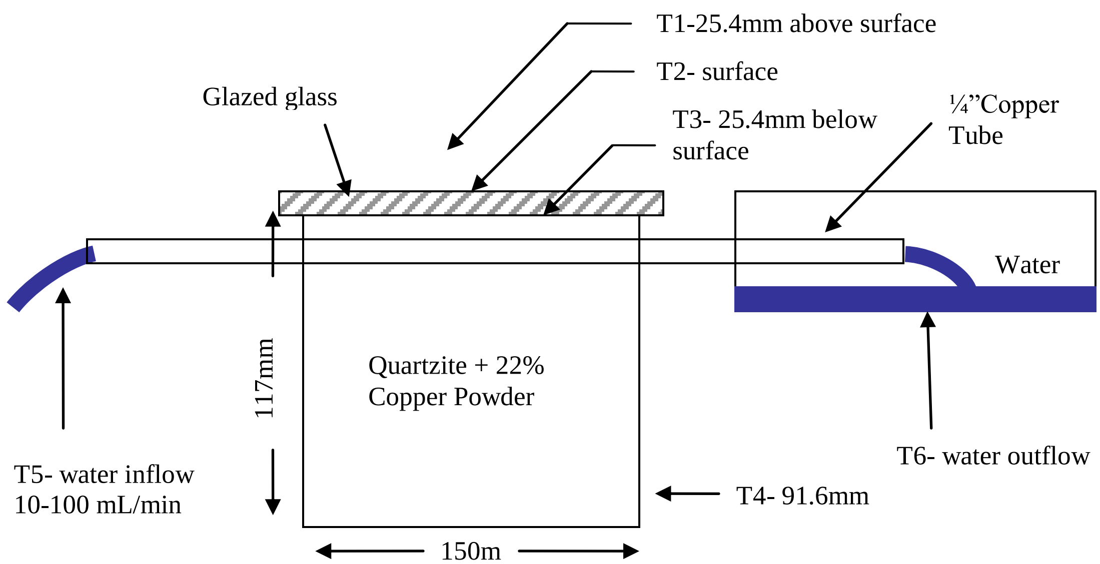

Figure 20: Schematic Quartzite w/ 22% Copper and Glazed Glass

The sample labeled Case 8 is a sample made with quartzite aggregate enhanced with 22% copper powder with a piece of glazed glass placed over the sample during testing. There is a ¼" copper pipe in the sample 1" below the surface. The system had ice-water pumped at a flow rate 1mL/min, then 5mL/min, similarly at 8, 10, 20, 30, 40, 50, 60, 70, 80, 90, and 100mL/min.

Case 9: Quartzite w/ 22% Copper and Acrylic Paint

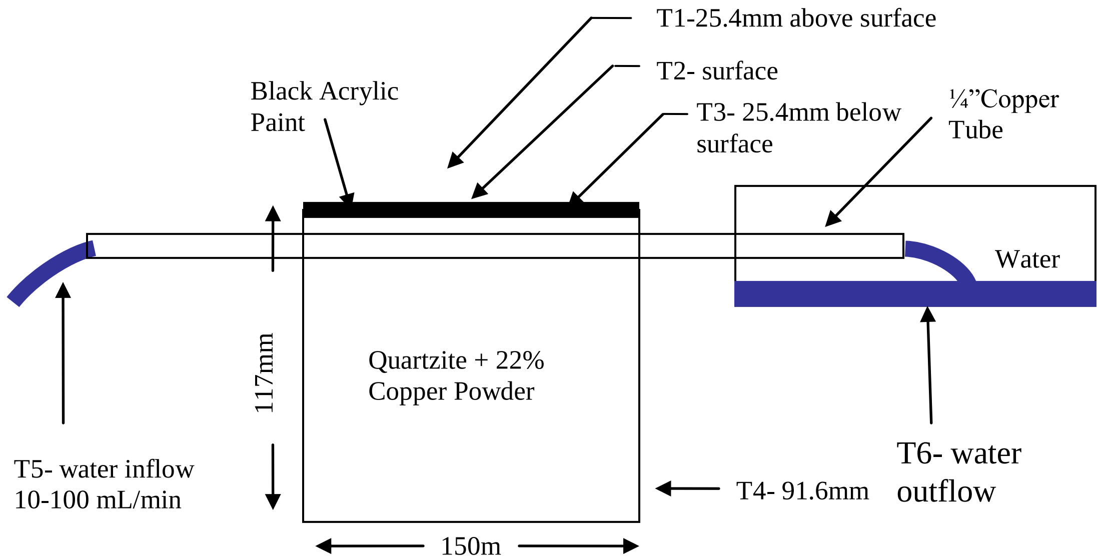

Figure 21: Schematic of Quartzite w/ 22% Copper and Acrylic Paint

The sample labeled Case 9 is a sample made with quartzite aggregate enhanced with 22% copper powder with a coat of black acrylic paint on the sample during testing. There is a ¼" copper pipe in the sample 1" below the surface. The system had ice-water pumped at a flow rate 1mL/min, then 5mL/min, similarly at 8, 10, 20, 30, 40, 50, 60, 70, 80, 90, and 100mL/min.

Case 10: Quartzite w/ 30% Aluminum

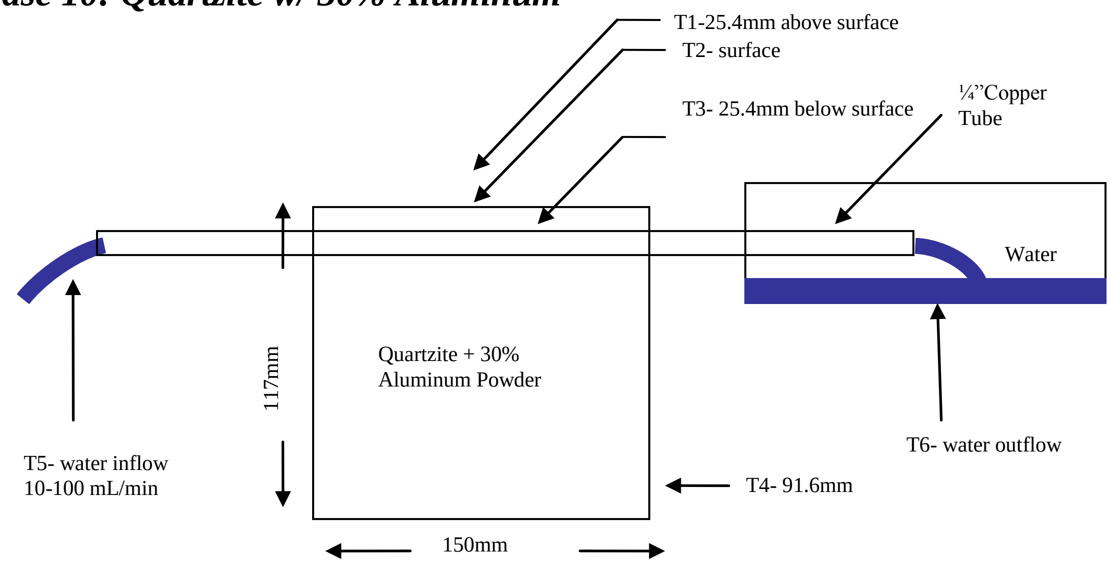

Figure 22: Schematic of Quartzite w/ 30% Aluminum

The sample labeled Case 10 is a sample made with quartzite aggregate enhanced with 30% aluminum powder with a ¼" copper pipe in the sample 1" below the surface. The system had ice-water pumped at a flow rate 1mL/min, then 5mL/min, similarly at 8, 10, 20, 30, 40, 50, 60, 70, 80, 90, and 100mL/min.

Case 11: Quartzite w/ 30% Aluminum and Glazed Glass

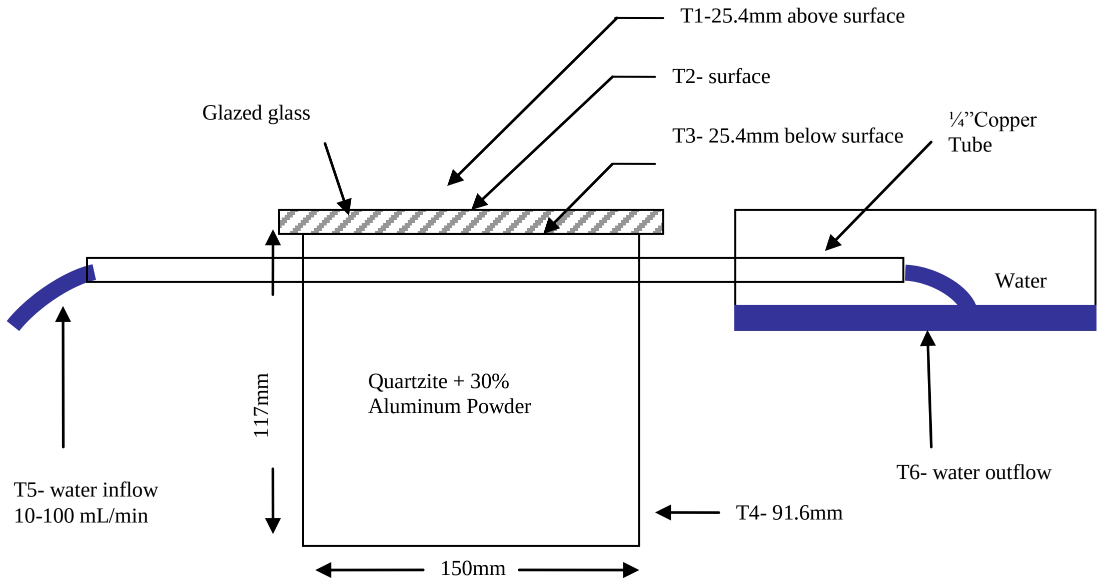

Figure 23: Schematic of Quartzite w/ 30% Aluminum and Glazed Glass

The sample labeled Case 11 is a sample made with quartzite aggregate enhanced with 30% aluminum powder with a piece of glazed glass placed on top during testing. There is a ¼" copper pipe in the sample 1" below the surface. The system had ice-water pumped at a flow rate 1mL/min, then 5mL/min, similarly at 8, 10, 20, 30, 40, 50, 60, 70, 80, 90, and 100mL/min.

Case 12: Quartzite w/ 30% Aluminum w/ Glass Asphalt

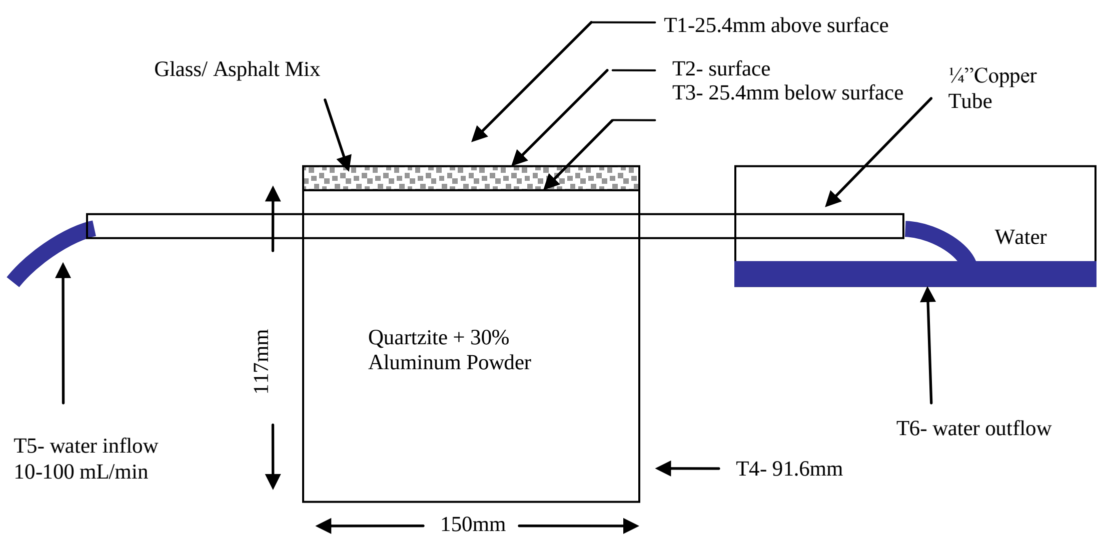

Figure 24: Schematic of Quartzite w/ 30% Aluminum w/ Glass Asphalt

The sample labeled Case 12 is a sample made with quartzite aggregate enhanced with 30% aluminum powder with a layer of a mixture of crushed glass and PG64-28 asphalt. There is a ¼" copper pipe in the sample 1" below the surface. The system had ice-water pumped at a flow rate 1mL/min, then 5mL/min, similarly at 10, 20, 40, 60, 80 and 100mL/min.

Case 13: Quartzite w/ 75%RAP

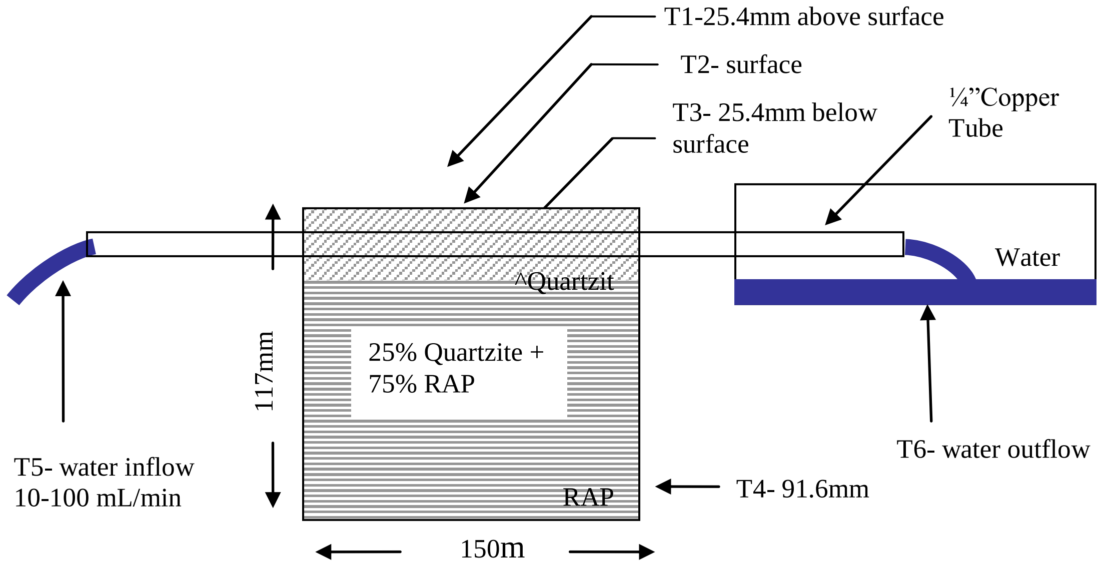

Figure 25: Schematic of Quartzite w/ 75% RAP

The sample labeled Case 13 is a sample made with 75% RAP (recycled asphalt product) on the bottom layers and 25% quartzite aggregate on the top layers. There is a ¼" copper pipe in the sample 1" below the surface. The system had ice-water pumped at a flow rate 1mL/min, then 5mL/min, similarly at 10, 20, 40, 60, 80 and 100mL/min.

Case 14: 100% RAP

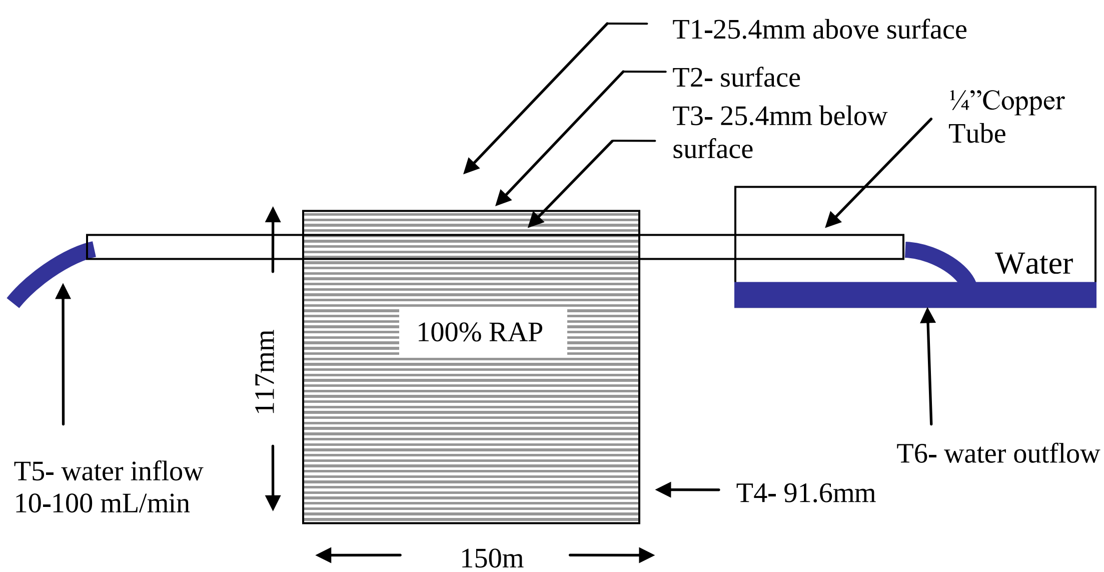

Figure 26: Schematic of 100% RAP

The sample labeled Case 14 is a sample made with 100% RAP (recycled asphalt product). There is a ¼" copper pipe in the sample 1" below the surface. The system had ice-water pumped at a flow rate 1mL/min, then 5mL/min, similarly at 10, 20, 40, 60, 80 and 100mL/min.

Case 15: 50% Quartzite, 50% RAP

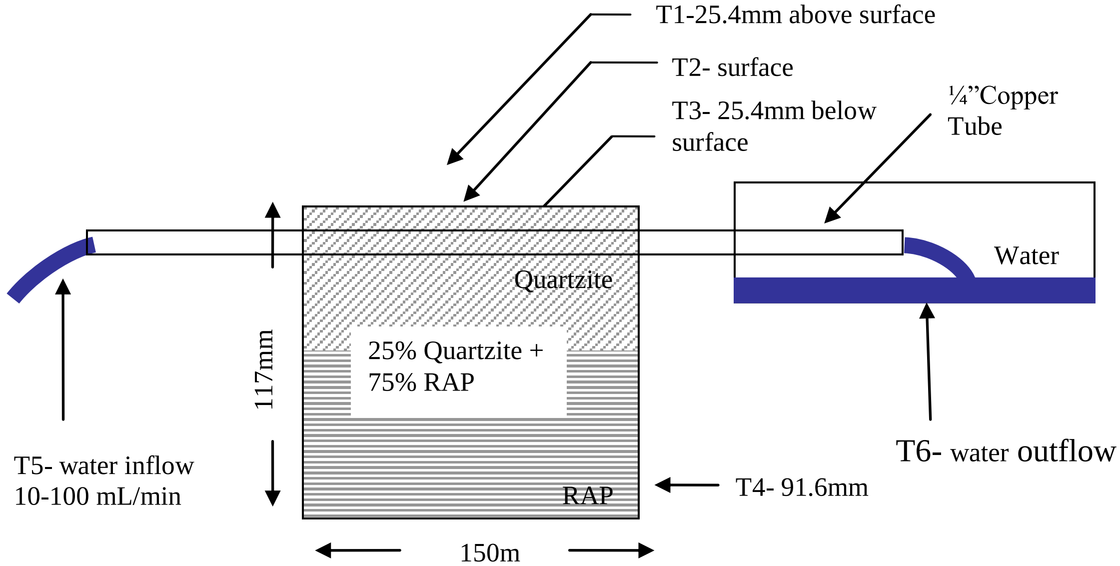

Figure 27: Schematic of 50% RAP and 50% Quartzite

The sample labeled Case 15 is a sample made with 50% RAP (recycled asphalt product) on the bottom layers and 50% quartzite aggregate on the top layers. There is a ¼" copper pipe in the sample 1" below the surface. The system had ice-water pumped at a flow rate 1mL/min, then 5mL/min, similarly at 10, 20, 40, 60, 80 and 100mL/min.

Case 16: 100% Wrentham Mix

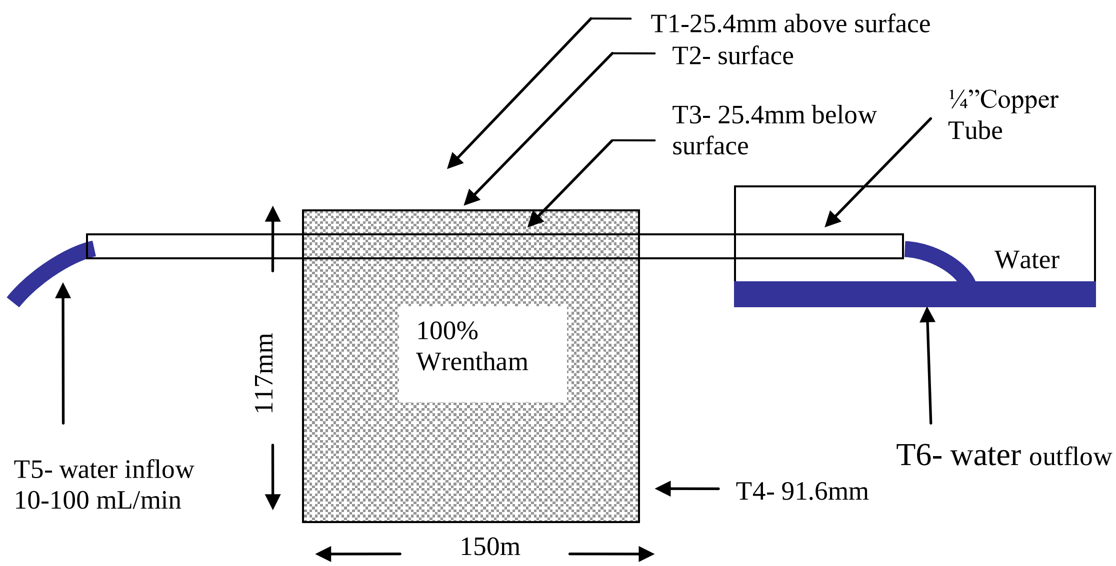

Figure 28: Schematic of 100% Wrentham Mix

The sample labeled Case 16 is a sample made with 100% aggregates from Wrentham. There is a ¼" copper pipe in the sample 1" below the surface. The system had ice-water pumped at a flow rate 1mL/min, then 5mL/min, similarly at 10, 20, 40, 60, 80 and 100mL/min.

Case 17: 67% Quartzite, 33% Limestone

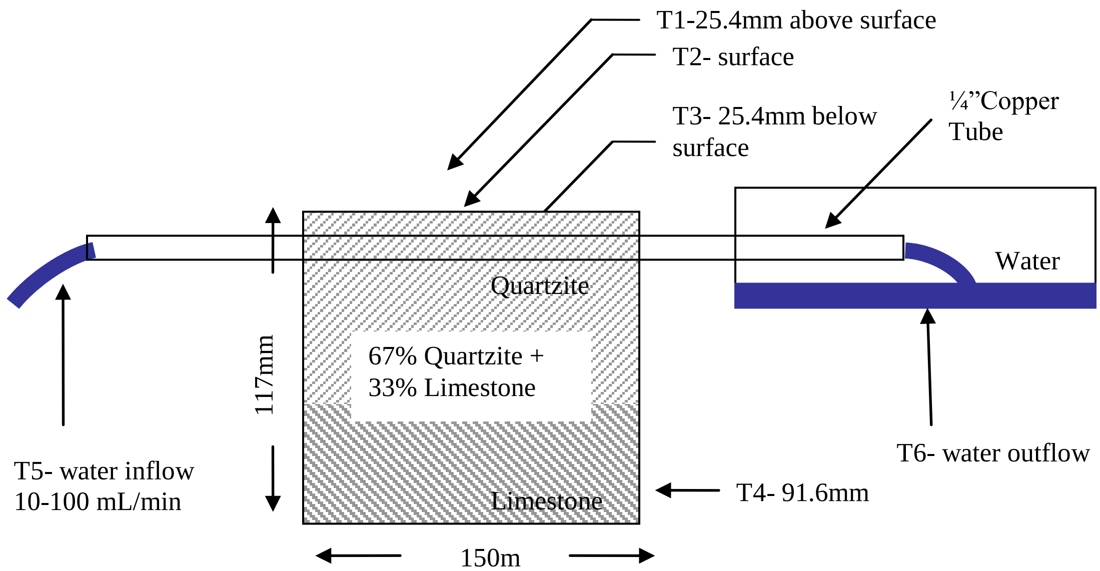

Figure 29: Schematic 67% Quartzite and 33% Limestone

The sample labeled Case 17 is a sample made with 67% quartzite aggregates on the top layers and 33% limestone on the bottom. There is a ¼" copper pipe in the sample 1" below the surface. The system had ice-water pumped at a flow rate 1mL/min, then 5mL/min, similarly at 10, 20, 40, 60, 80 and 100mL/min.

Slab Tests

The next phase of testing for this projected consisted of constructing 2 large slabs measuring 3'x6'. One of the slabs is comprised of 2/3 quartzite aggregates with a base of 1/3 granite (fromWrentham) mix, with a depth of 4.7". This slab will be referred to as the quartzite slab. The second slab is made entirely of the Wrentham mix and has a depth of 5.3".

A system of ½"copper piping was assembled and placed on the second to last lift of pavement during the assembly of the slabs. It was then covered with pavement to be approximately one inch below the surface. One inch was the depth that reached the highest temperature in the preliminary laboratory testing. The pipes ran 3 across in the narrow direction and one down the middle across the 6 foot span.

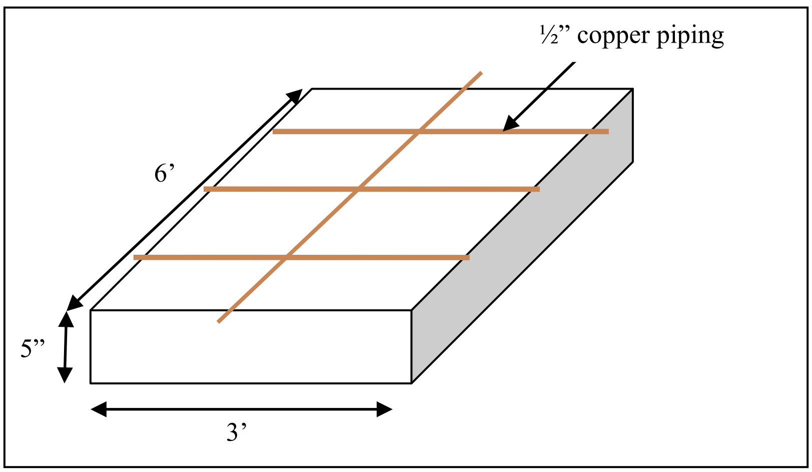

Figure 30: Simple Slab Dimension Schematic

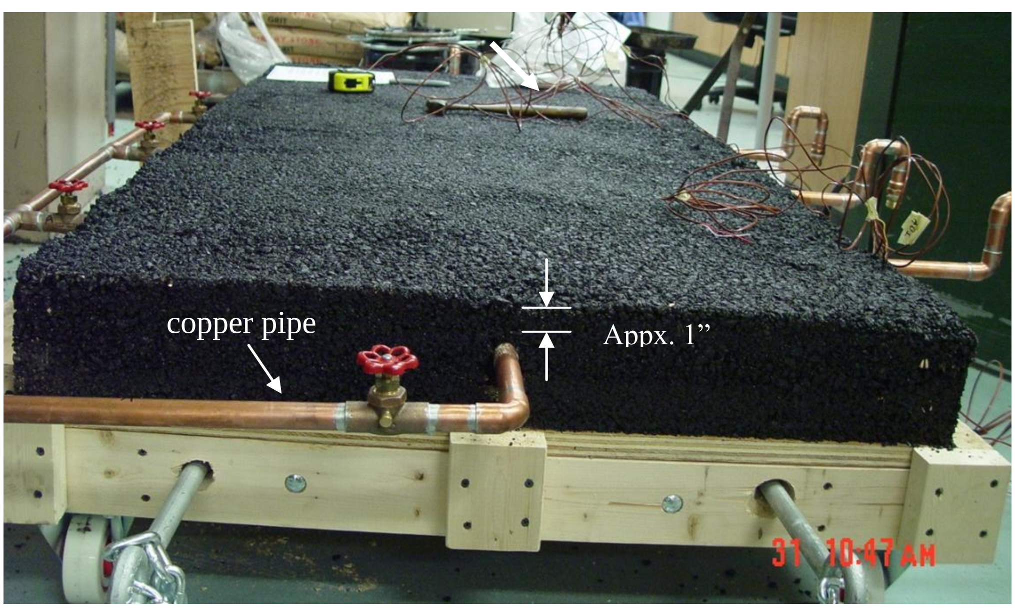

Figure 31: Slab with Copper Pipe Depth

Asphalt mix was poured on top of the copper frame so that the pipes would be beneath the surface. A steel barrel roller manufactured in the lab at WPI was used to compact both of the slab samples.

Figure 32: Compacting Slab

Unlike the previous small samples tested inside the laboratory, the slabs were tested outside in the sunlight. Water was run though various pipes at a range of flow rates from1-4L/min. When testing with water flowing through the center pipes in both directions, the flow rates ranged from 300-1000mL/min, but adjusting at different times. At first both were started with them same flow rates, and then adjusted to determine if the rate would make a difference for either. Also noted during testing were the ambient temperature, solar radiation, and wind speed.

Slab Test Descriptions

There were 8 test total run on the slab samples:

Test 1 was a steady state test of the Wrentham (granite) mix heated up with no water flow.

Test 2 was a steady state test of the quartzite mix heated up with no water flow.

Test 3 was testing of the Wrentham mix slab with flow rates of 500mL/min and 1000mL/min at both center pipes (3' and 6'), and flow rates of 300ml and 1000mL at each center pipe.

Test 4 was testing of the quartzite mix slab with flow rates of 500mL/min and 1000mL/min at both center pipes (3' and 6'), and flow rate of 300ml and 1000mL at each center pipe.

Test 5 was a test of the Wrentham mix slab with flow rates of 1000, 2000, 3000, and 4000 mL/min at both center pipes (3' and 6').

Test 6 was a test of the quartzite mix slab with flow rates of 1000, 2000, 3000, and 4000 mL/min at both center pipes (3' and 6').

Test 7 was a steady state testing of the Wrentham mix slab with 1/3 acrylic paint on surface being heated up with no water flow.

Test 8 was a testing of the quartzite mix slab with flow rates of 1000, 2000, 3000, 4000mL at right end pipe and 1000mL/min at right and center pipes.

Results

Case 1: The all quartzite sample after testing with standing water for temperature increase yielded the following results:

The following graph displays the temperature results of each of the thermocouples in the samples while testing over 6 hours. Thermocouple 2, located on the surface, reached the greatest temperature difference reaching a high temperature of about 70°C. The temperature increase of water over the duration of the testing was 10.13°C.

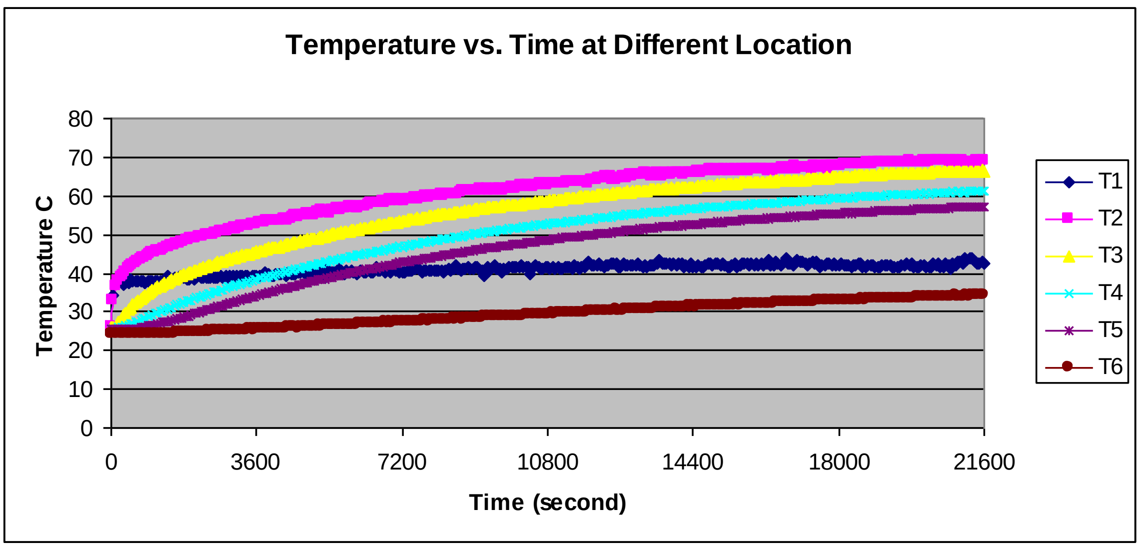

Figure 33: Temperature vs. Time for Quartzite Sample

Case 2: The all limestone sample after testing with standing water only yielded the following results:

The following graph displays the temperature results of each of the thermocouples in the samples while testing over 6 hours. Thermocouple 2, located on the surface, reached the greatest temperature difference reaching a high temperature of about 70°C. The temperature increase of water over the duration of the testing was 5.02°C.

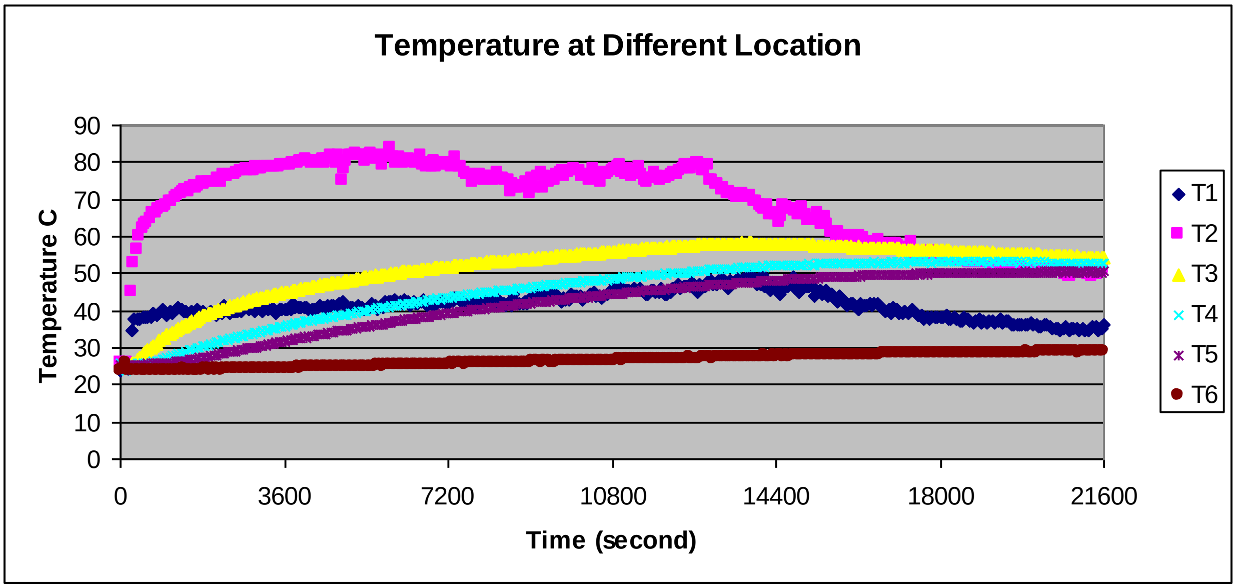

Figure 34: Temperature vs. Time for Limestone Sample

Note: The irregular pattern of T2 is most likely due to the improper fixing of the thermocouple on the sample.

Case 3: The all quartzite sample after testing with standing water and a piece of glass on the top of the surface of the sample yielded the following results:

The following graph displays the temperature results of each of the thermocouples in the samples while testing over 6 hours. Thermocouple 3, located on e inch beneath the surface, reached the greatest temperature difference reaching a high temperature of about 73°C. The temperature increase of water over the duration of the testing was 10.47°C.

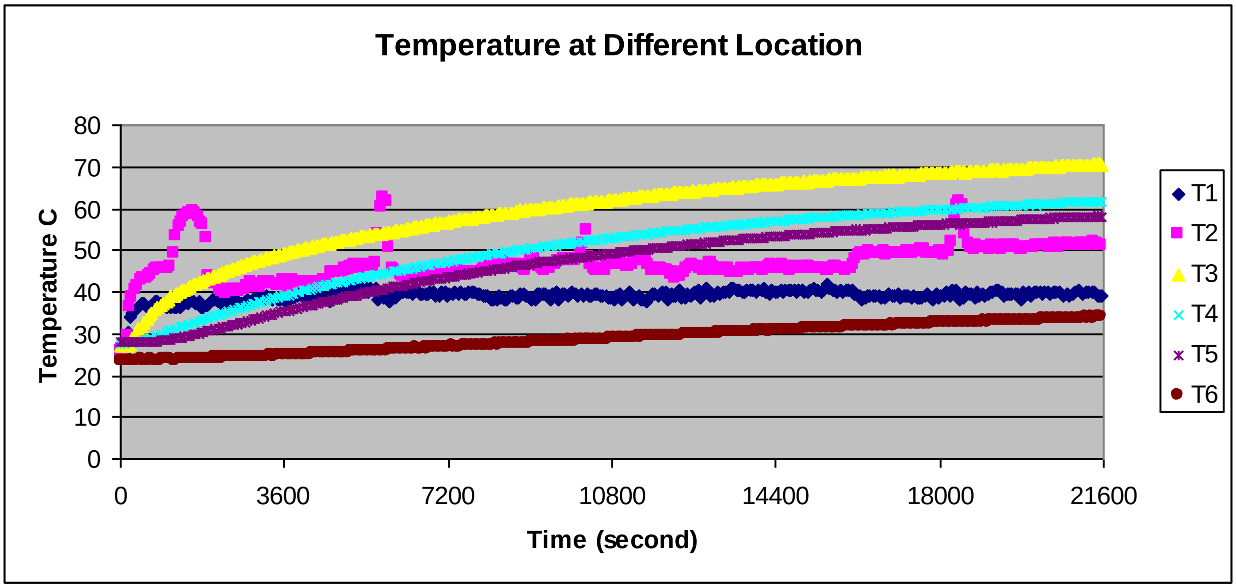

Figure 35: Temperature vs. Time Quartzite w/ Glass Top

Note: The erratic behavior of T2 (thermocouple 2) in this graph is suspected to be the result of a non-secured thermocouple on the surface of the sample.

Case 4: The quartzite sample after testing with ice water and 3mL flow and steady state water yielded the following results:

The following graph displays the temperature results of each of the thermocouples in the samples while testing over 6 hours. Thermocouple 3, located one inch beneath the surface, reached the greatest temperature averaging around 63°C. The temperature increase of water over the duration of the testing was 28.27465.

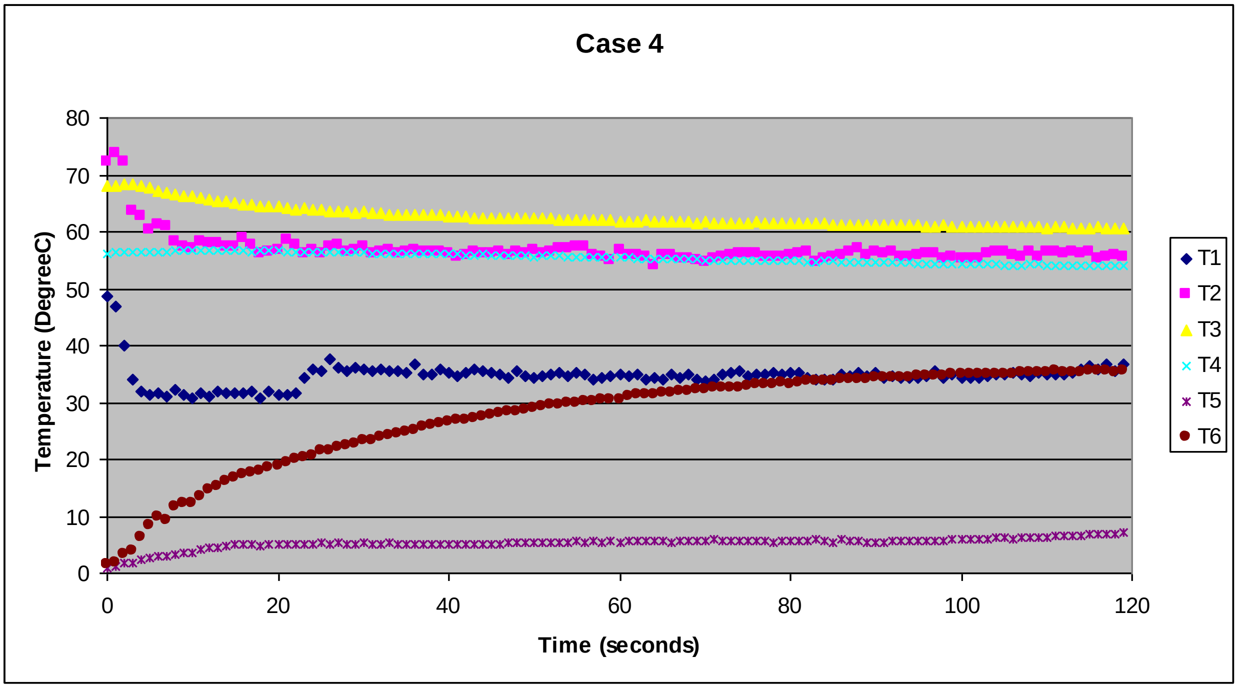

Figure 36: Temperature vs. Quartzite Sample w/ Ice Water and 3mL Steady Flow

Note: The inconsistency in T1 during the beginning of testing is thought to be the result of drafts of air disrupting the ambient air temperature.

The inconsistency in T2 for the 10 minutes is thought be the result of an unsecured thermocouple.

Case 5: The quartzite sample after testing with water pumped through at 3ml flow yielded the following results:

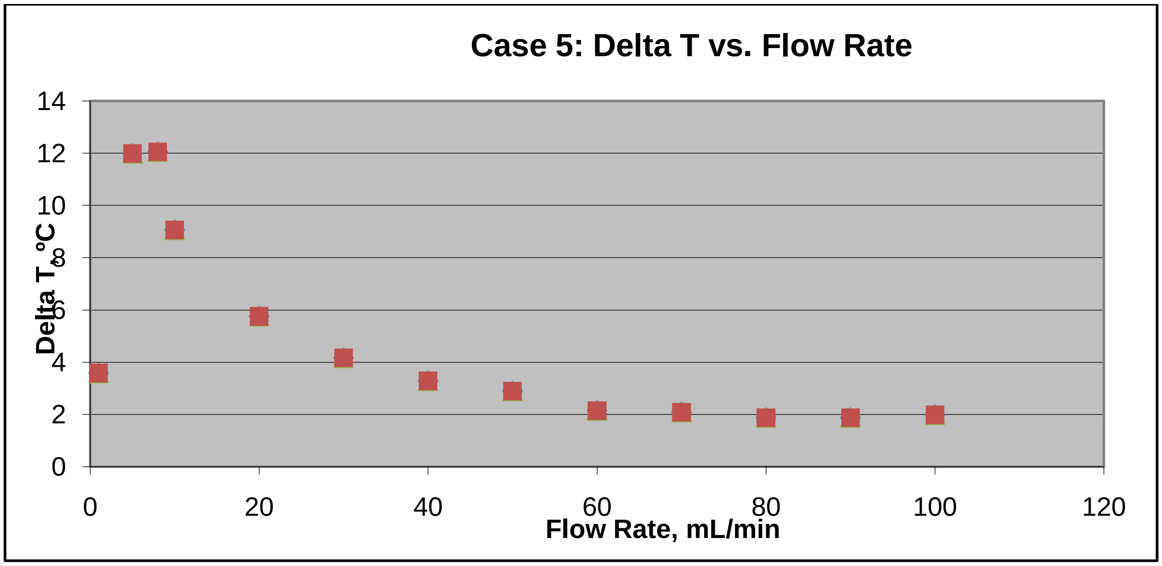

Figure 37: Case 5: Delta T vs. Flow Rate

The graph of ΔT vs. time shows that as flow rate increased from 1mL/min to 100mL/min, the difference in temperature decreased. Therefore, a higher flow rate does not provide a greater difference in temperature.

Case 6: The quartzite sample after testing with ice water and varying flow rates ranging from 10-100mL/min yielded the following results:

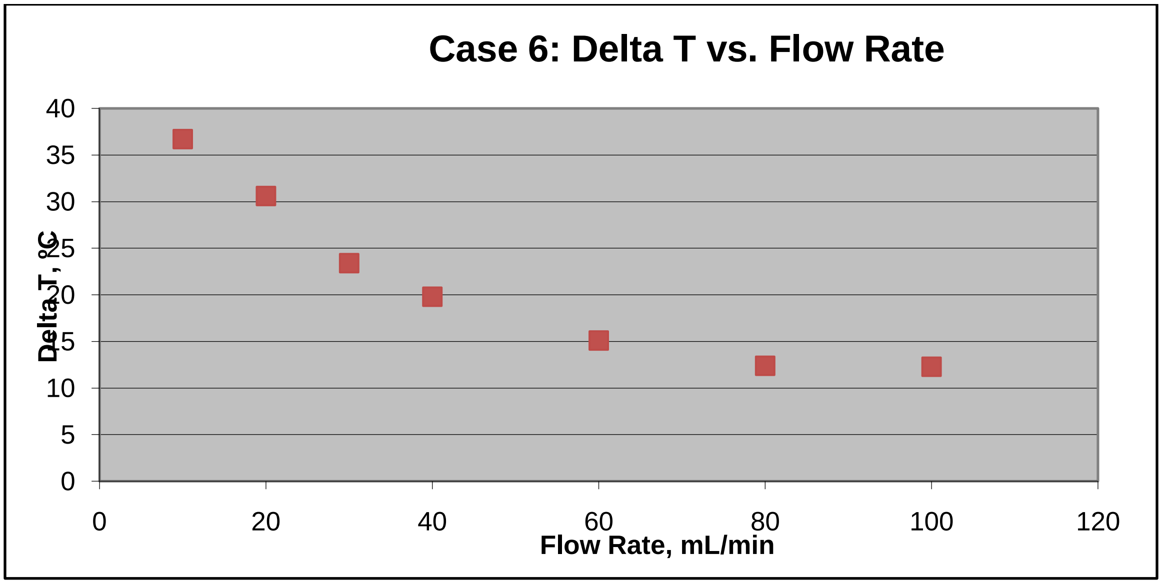

Figure 38: Case 6 Delta T vs. Flow Rate

The graph of ΔT vs. time shows that as flow rate increase, the difference in temperature decreases. The greatest ΔT was 36.7 °C which was at a rate of 10mL/min

Flow Rate 10mL

The following graph displays the temperature results of each of the thermocouples in the samples while testing over 6 hours. Thermocouple 3, located one inch beneath the surface, reached the greatest temperature averaging around 97°C. The temperature increase of water over the duration of the testing was 36.7101.

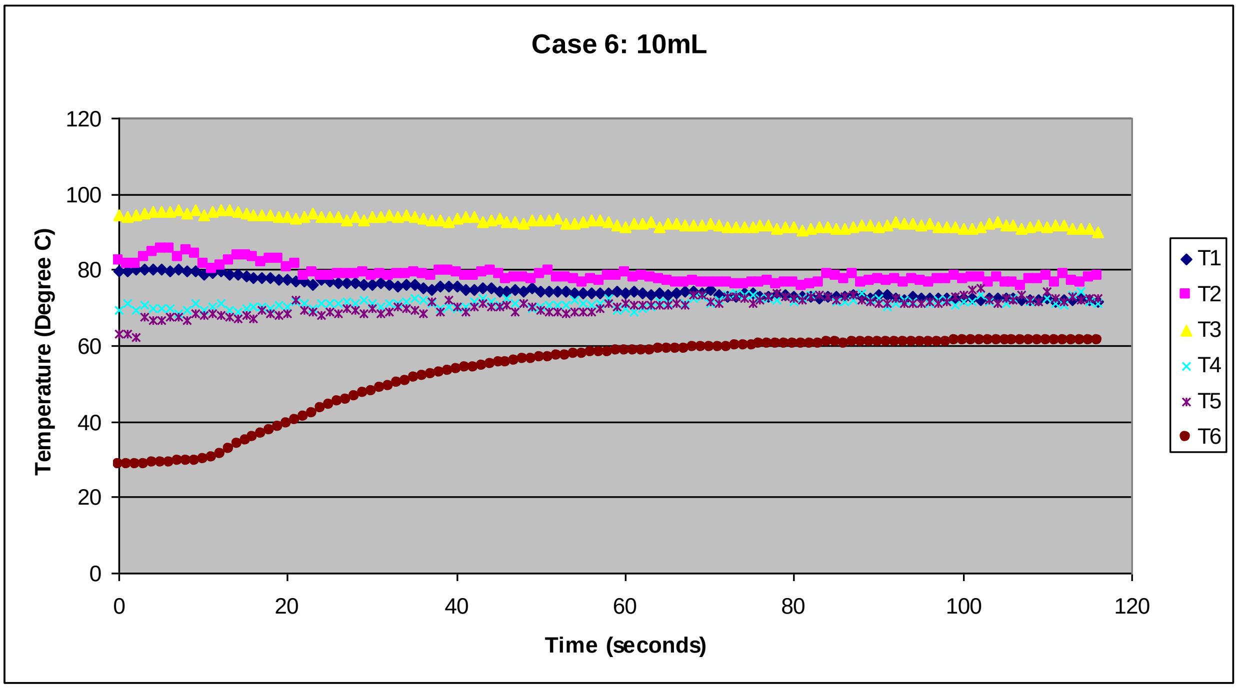

Figure 39: Temperature vs. Time, Case 6: 10mL/min

Case 7: The quartzite sample with 22% Cu powder mixed throughout the sample after testing with water at various flow rates from 1ml up to 100ml yielded the following results:

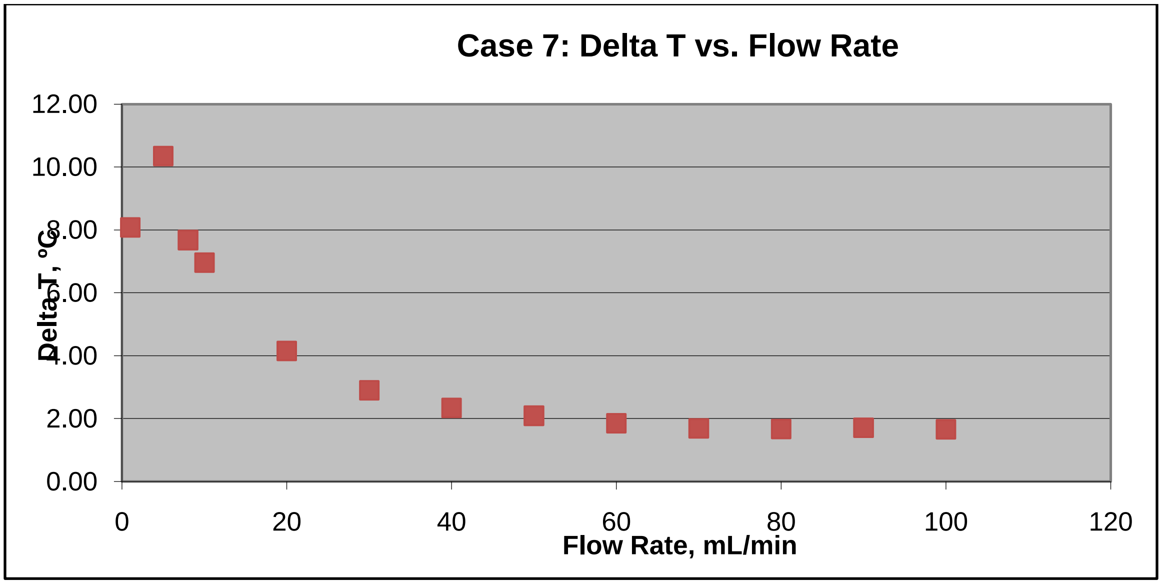

Figure 40: Case 7: Delta T vs. Flow Rate

The graph of ΔT vs. Time for Case 7 shows that as the flow rate increase, the temperature decreases. The highest temperature difference was achieved at 5mL/min and was a difference of 10.35°C. This concludes that lower flow rates produce greater temperature differences which are advantageous.

Case 8: The quartzite sample with 22% Cu powder and a glazed piece of glass the sample after testing with water at various flow rates from 1ml up to 100ml yielded the following results:

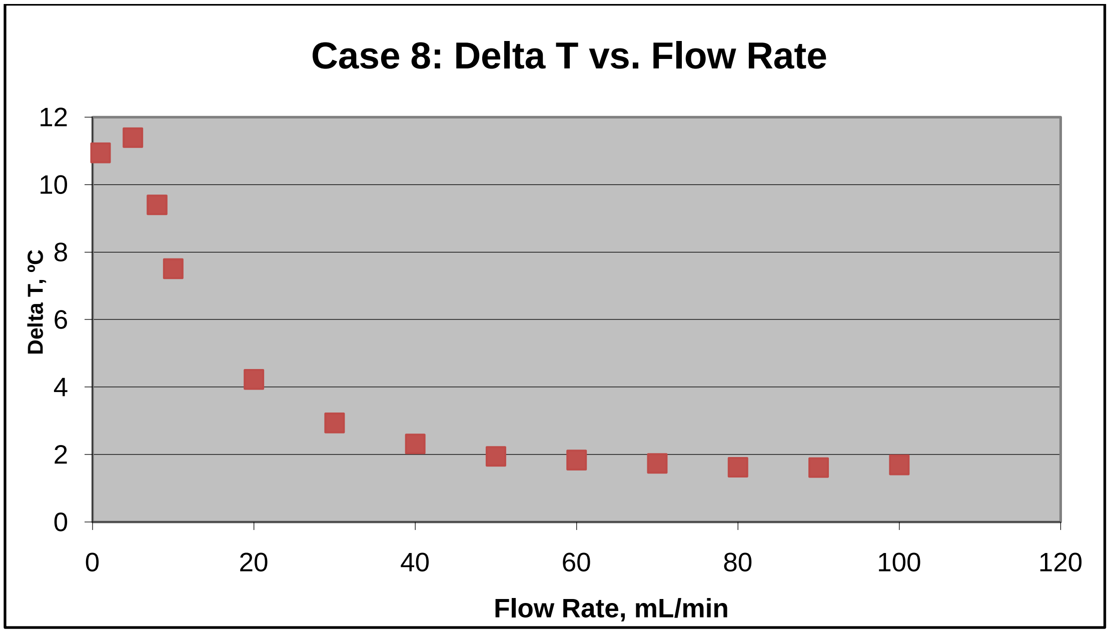

Figure 41: Case 8: Delta T vs. Flow Rate

The graph of ΔT vs. Time shows that as flow rate increase, the temperature decreases. The highest temperature difference was found at 5mL/min and was 11.39°C. The lower flow rate produces a higher temperature difference.

Case 9: The quartzite sample with 22% Cu powder and acrylic paint painted on the surface of the sample after testing with water at various flow rates from 1ml up to 100ml yielded the following results:

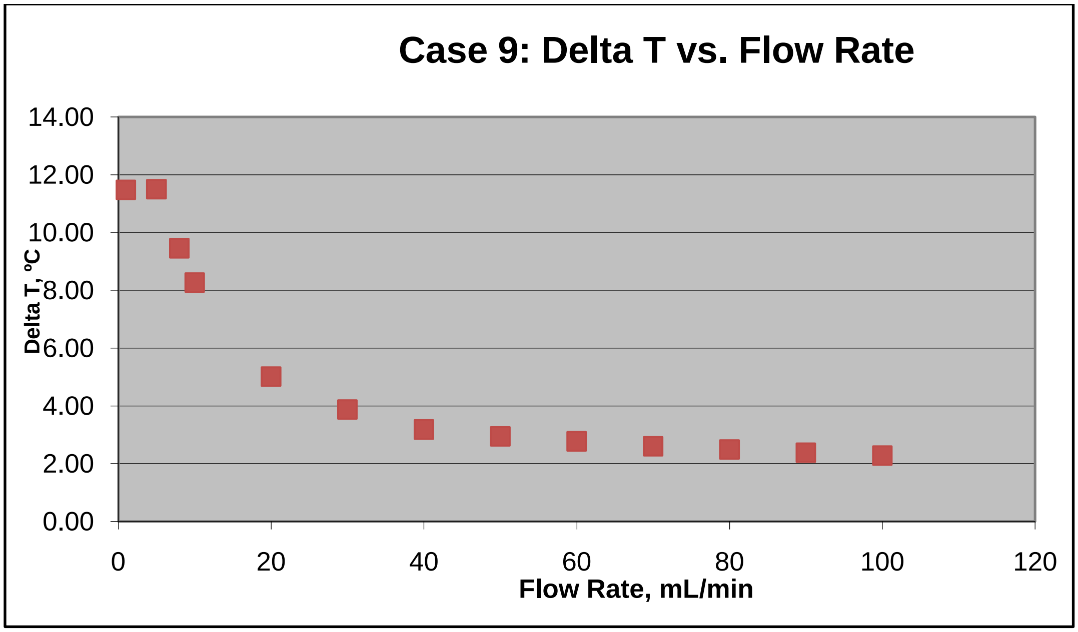

Figure 42: Case 9: Delta T vs. Flow Rate

The graph of ΔT vs. time for case 9 shows that temperature decreases as flow rate progresses. The optimal flow rate for this test was 5mL/min producing a temperature difference of 11.5°C.

Case 10: The quartzite sample with 30% aluminum powder mixed throughout the sample, after testing with water at various flow rates from 1ml up to 100ml yielded the following results:

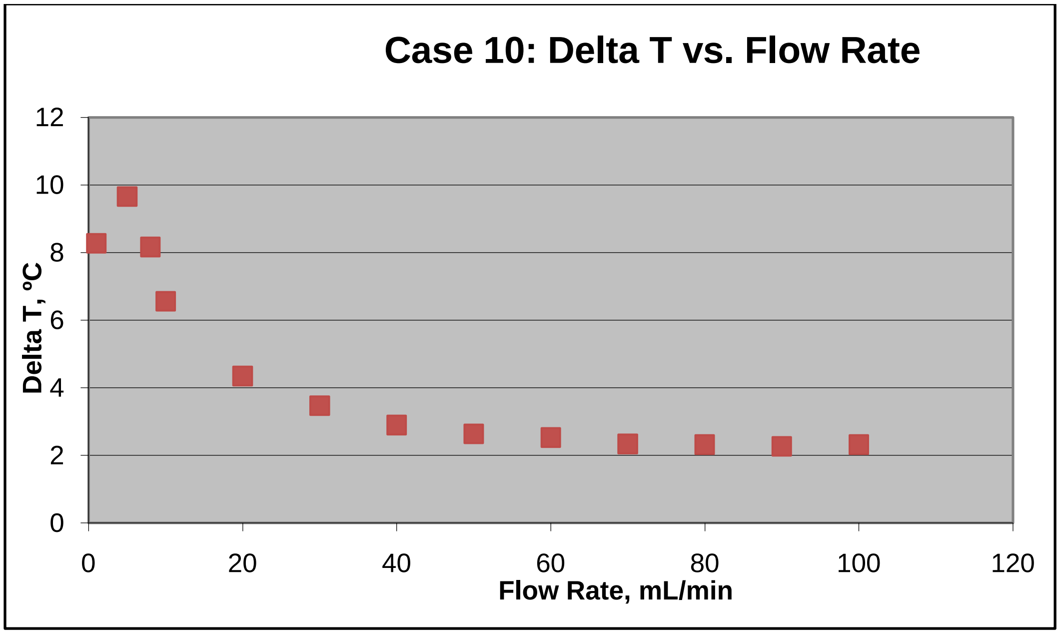

Figure 43: Case 10: Delta T vs. Flow Rate

The graph of case 10 shows that as flow rate increase, the difference in temperature decreases. The greatest temperature difference was 9.66mL/min achieved at 5mL/min. This demonstrates that lower flow rates produce greater temperature differences.

Case 11: The quartzite sample with 30% aluminum powder and a coated glass placed on top the sample, after testing with water at various flow rates from 1ml up to 100ml yielded the following results:

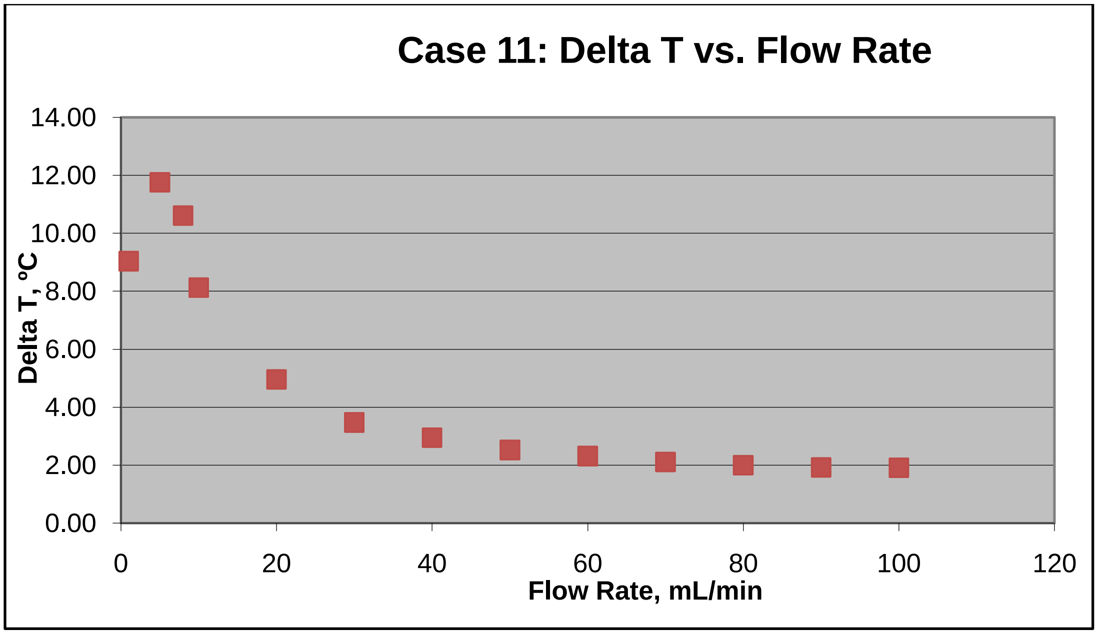

Figure 44: Case 11: Delta T vs. Flow Rate

The graph of case 11 shows that as flow rate, increase, the difference in temperature decreases. The greatest temperature difference was 11.76 which were achieved at 5mL/min.

Case 12: The quartzite sample with 30% aluminum powder and a glass and asphalt mix placed on top the sample, after testing for 67 minutes with water at each various flow rates from 1ml up to 100ml yielded the following results:

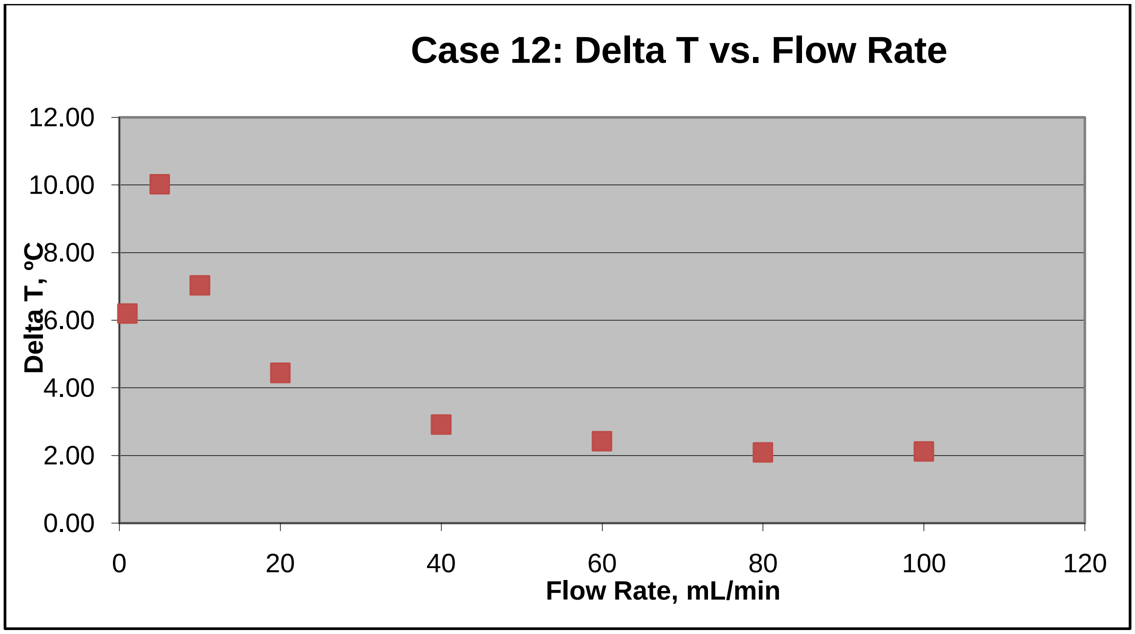

Figure 45: Case 12: Delta T vs. Flow Rate

The graph of Delta T vs. time for case 12 shows that as flow rate increases, the temperature difference decreases. There temperature difference for the first data point is slightly lower. This is suspected to be due to the face that a flow rate of 1mL/min is so low that it makes it difficult to create a temperature difference.

Case 13: The sample with 75% RAP and 25% quartzite after testing with water at various flow rates from 1ml up to 100ml yielded the following results:

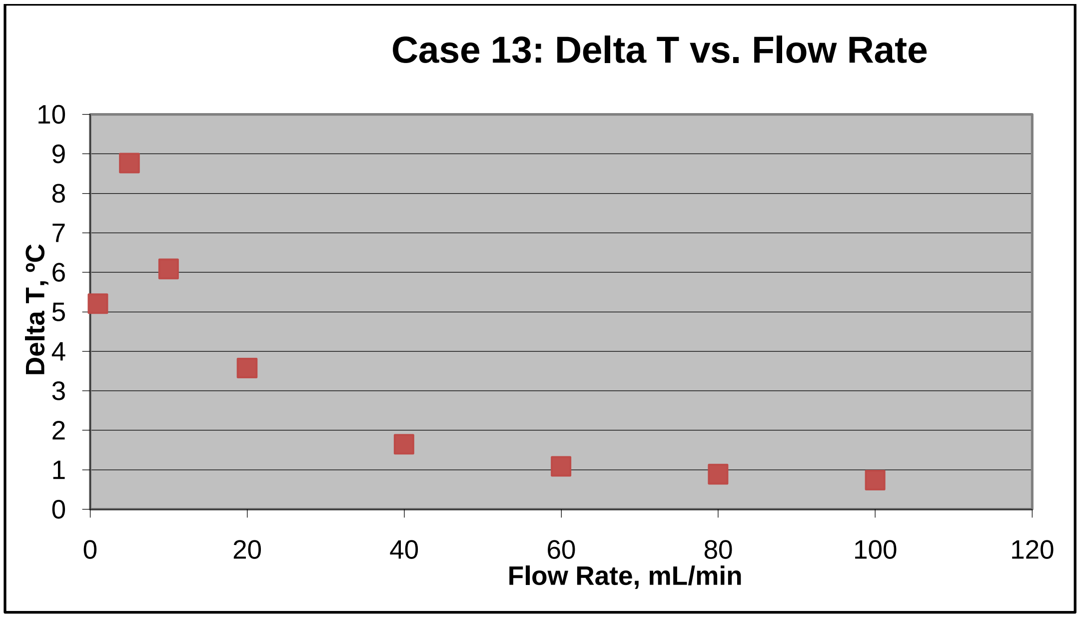

Figure 46: Case 13: Delta T vs. Flow Rate

The graph of ΔT vs. time for case 13 shows that as flow rate increase, the difference in temperature decreases. The greatest temperature difference was 8.77°C and was achieved at a flow rate of 5mL/min.

Case 14: The RAP sample after testing with water at various flow rates from 1ml up to 100ml for 21 minutes yielded the following results:

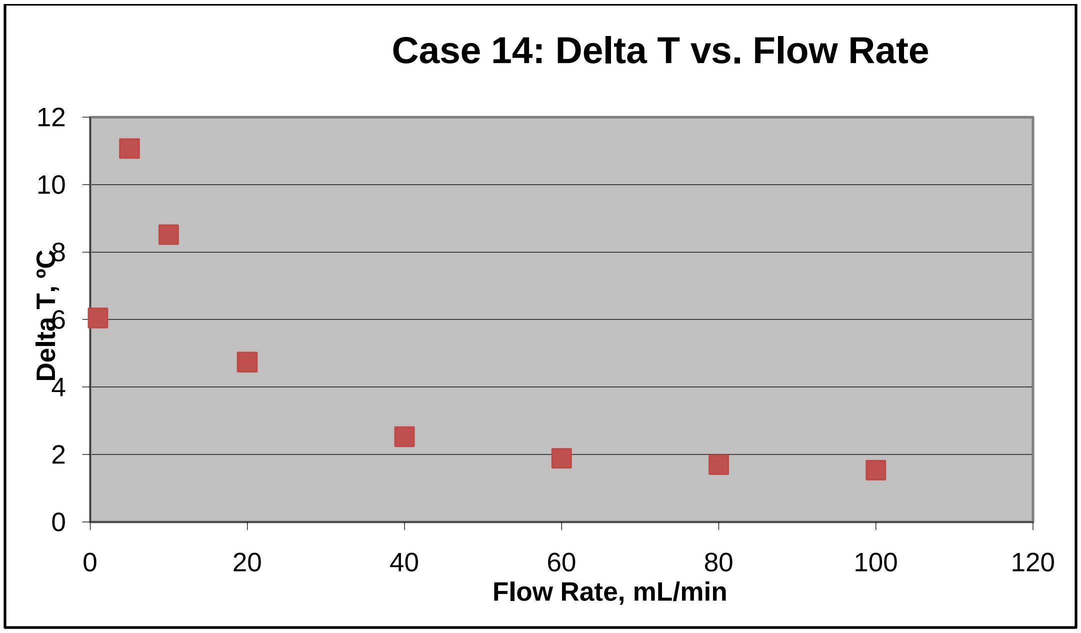

Figure 47: Case 14: Delta T vs. Flow Rate

The graph of ΔT vs. time shows that as flow rate increase, the difference in temperature decreases. This is seen as a trend in all but one point, the first which was at a rate of 1mL/min. Due to the flow rate being so low, it is suspected that the lack of flow was the cause of poor temperature difference. The greatest temperature difference was 11.07°C and was attained at 5mL/min.

Case 15: The sample with 50% RAP and 50% Quartzite after testing with water at various flow rates from 1ml up to 100mL produced the following results:

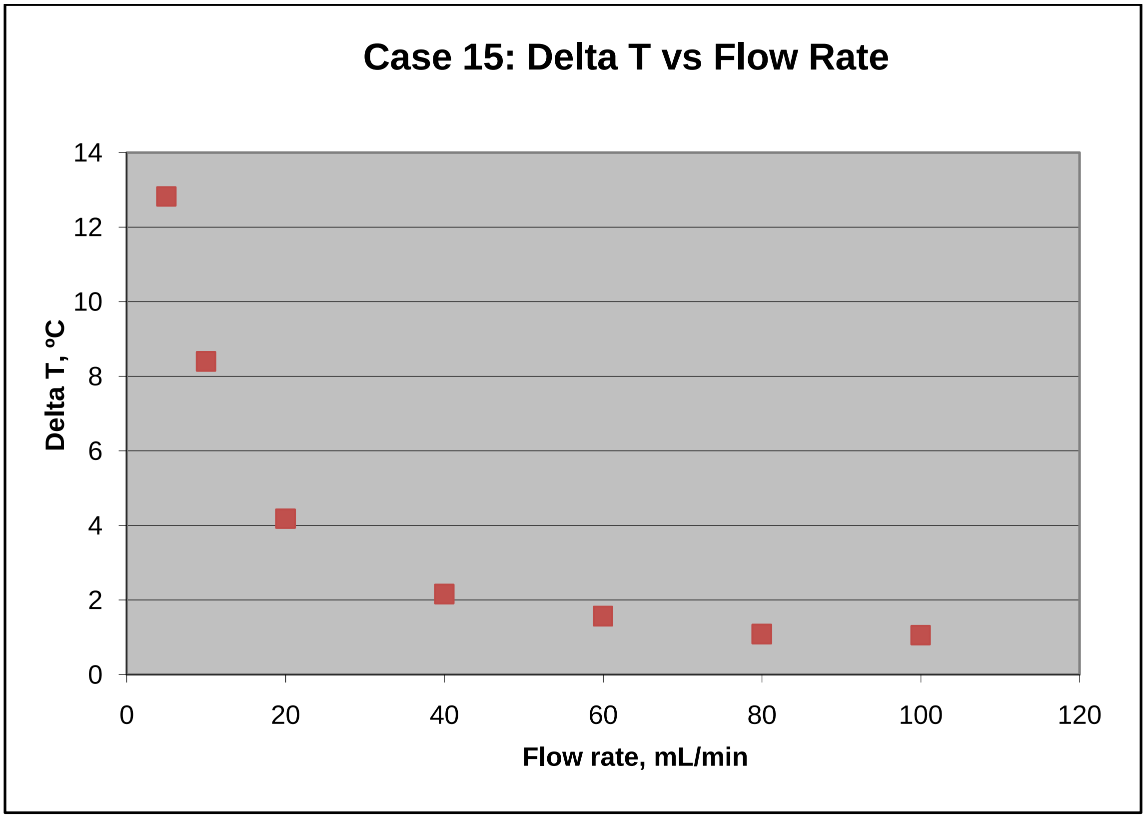

Figure 48: Case 15: Delta T vs. Flow Rate

The graph of ΔT vs. time for case 15 shows that as flow rate increases, the difference in temperature decreases. The greatest temperature difference for the sample was 12.82°C and was achieved at 5mL/min.

Case 16: The sample made of 100% Wrentham mix after testing with water at various flow rates from 1ml up to 100ml yielded the following results:

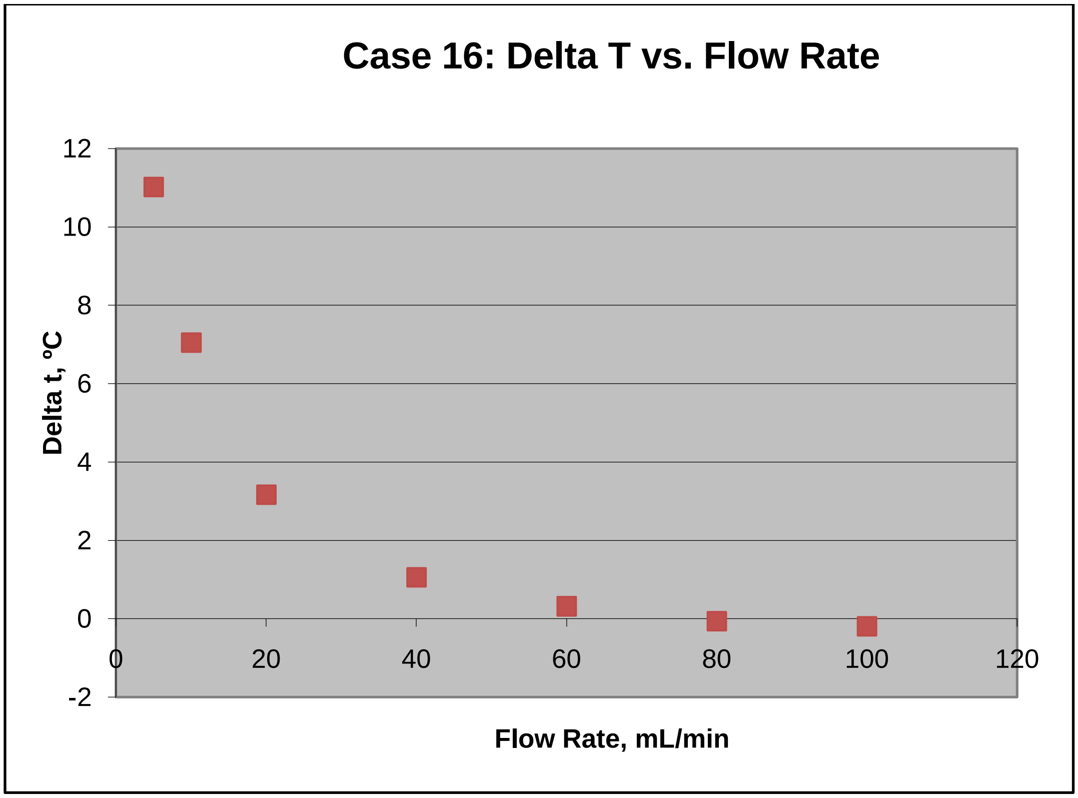

Figure 49: Case 15: Delta T vs. Flow Rate

The graph of ΔT vs. time for case 15 shows that as flow rate increases the temperature difference decreases. The last few data points actually show that there is no increase in temperature difference .The temperature actually decreased from its original temperature. This may be from a temperature change outside in addition to the minimal impact of the water flowing at such a high rate. The greatest temperature difference was 11.02 seen at 5ml/min.

Case 17: The sample made of 100% Wrentham mix after testing with water at various flow rates from 1ml up to 100ml yielded the following results:

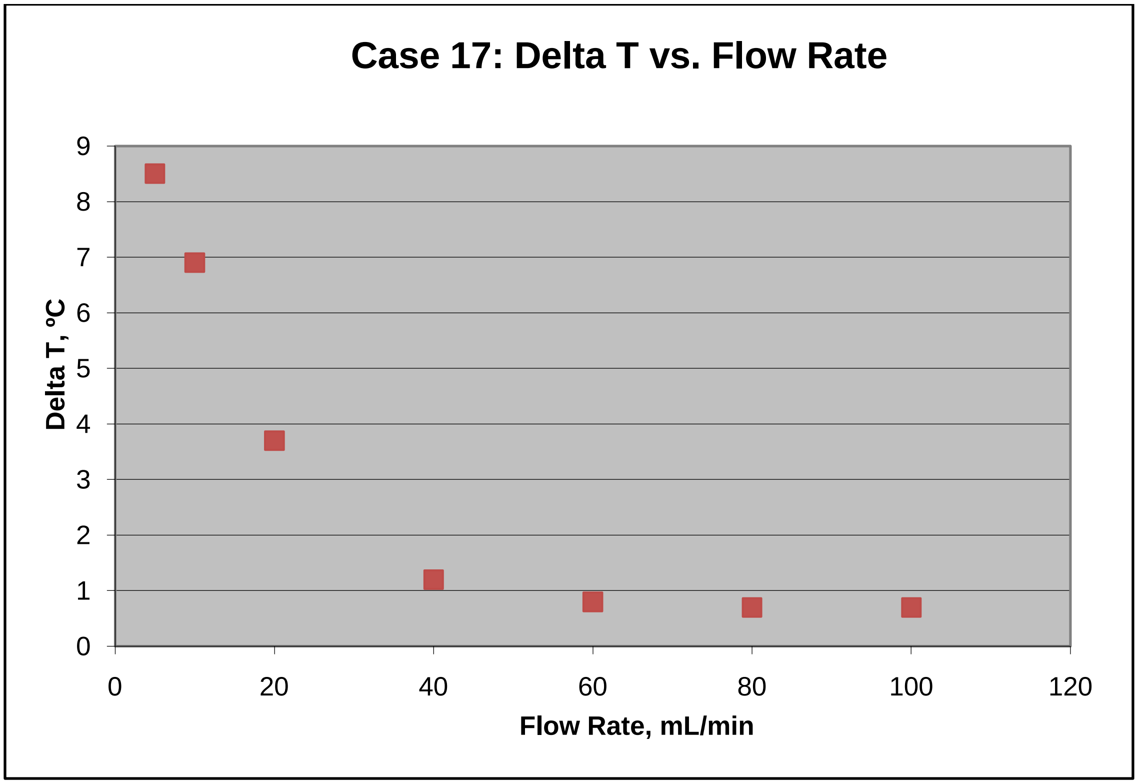

Figure 50: Case 17: Delta T vs. Flow Rate

The graph of ΔT vs. time shows that as flow rate, increase, the temperature difference decreases. The greatest temperature difference was 8.5°C and was seen at 5mL/min.

Comparisons

When comparing the temperature increase for each of the samples, it is easy to see that case 4 and 6 produced much greater heat increase reults. Case 4 was the the quartzite aggreagate tested with ice water. Case 6 was the HMA compiled with water flow. Overall quarzite produced the greatest temperature differences making it the dominant aggregate used for testing.

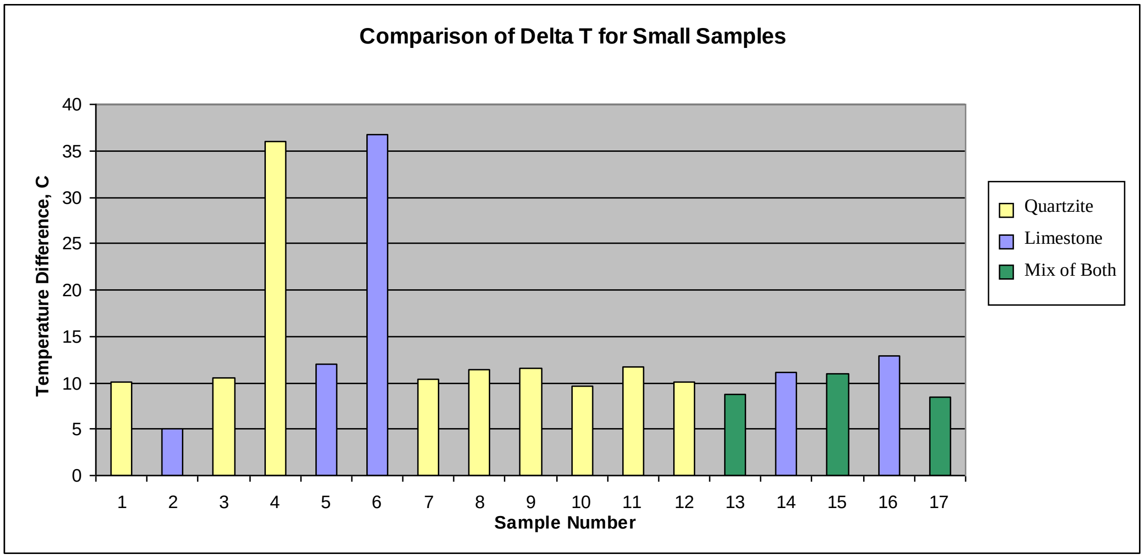

Figure 51: All Case Temperature Difference Comparison

The comparison of each of the 17 small samples shows that the quartzite samples, in yellow, create greater temperature difference overall. The blue denotes limestone samples and green represents mixes that were combinations of both aggregates.

Slab Testing Results

The first two tests that were run; one on the Wrentham mix slab, the other on the quartzite slab, were conducted to assess the setup and ensure all components were working properly. There was no data collected relevant to the results for this section of this report.

Test 3: Wrentham Mix

The result of the granite mix slab test with a flow rate of 500mL/min to 1000mL/min at both center pipes 3' and 6' and at a flow rate of 300 to 1000mL/min at each center pipe are as follows: The maximum temperature difference was found to be 7.18°C and was achieved at a flow rate of 300mL/min. The trend line shows that although the temperature differences fluctuated up and down, the difference in temperature was decreasing as flow rate increased. The lower the flow rate, the more optimal temperature difference can be achieved.

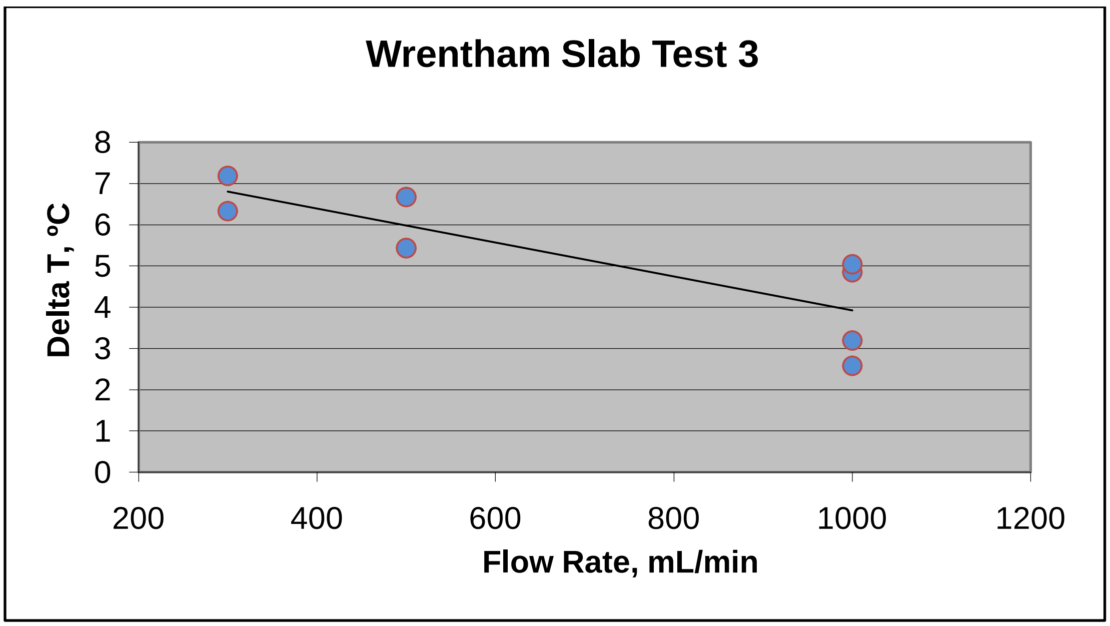

Figure 52: Wrentham Slab – Test 3

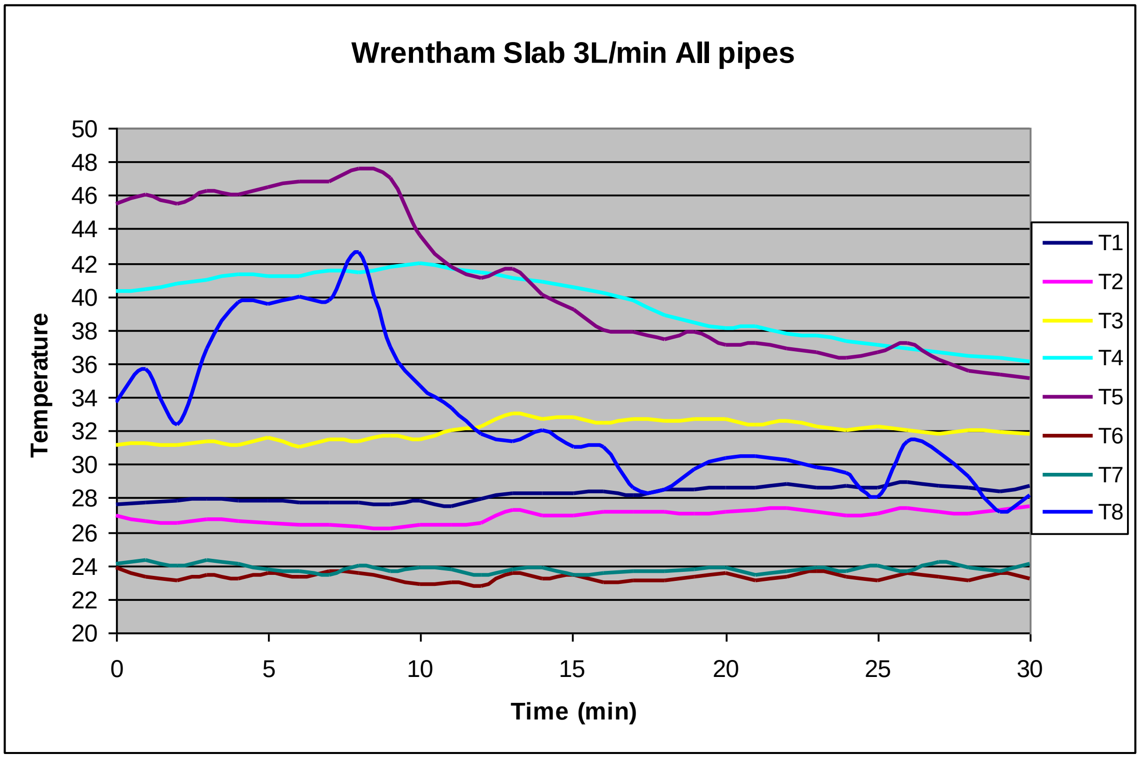

Figure 53: Thermocouple Data Test 3 – 3L/min

In the graph of the thermocouple data for the optimal flow rate, T4 is the thermocouple placed 1" below the surface. Thermocouples 5 and 8 are located on the surface. The irregular movement of these lines is suspected to be the result of non secure thermocouples on the surface of the sample.

Test 4: Quartzite Mix

The 2/3 quartzite and 1/3 granite slab was tested with a flow rate of 500mL/min and 1000mL/min at both center pipes. It was also tested at a flow rate of 300ml and 1000mL at each center pipe. The maximum temperature difference was 9.33°C and was achieved at 1000mL/min.

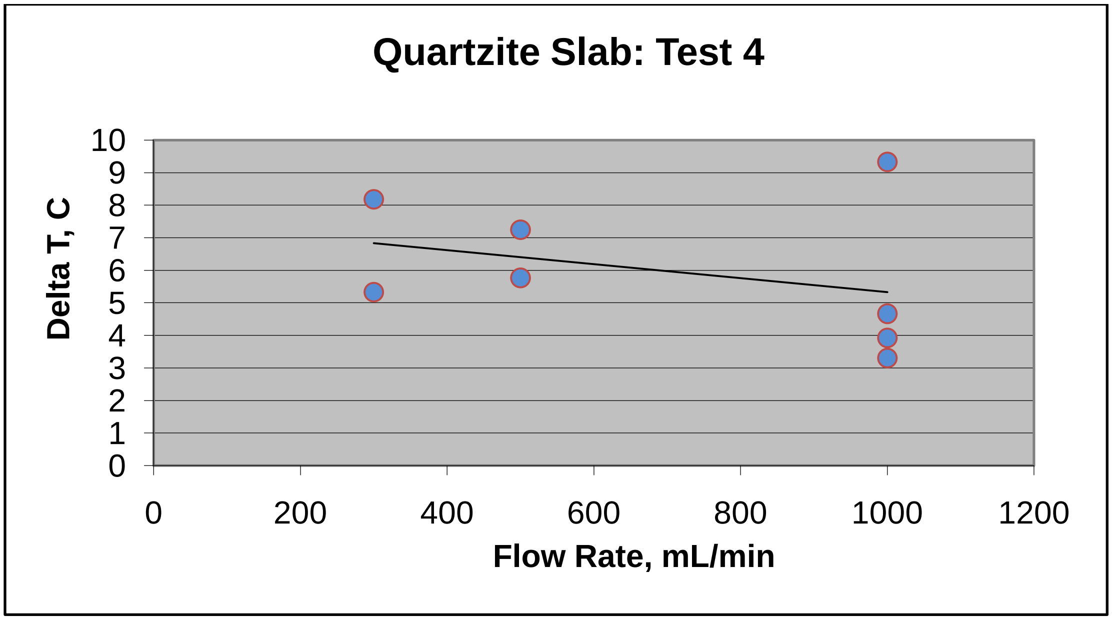

Figure 54: Quartzite Slab – Test 4

The graph of test 4 shows a trend that as also flow rate, increase, the temperature difference decrease.

Test 5: Wrentham Mix

The granite mix slab was test with a flow rate of 1000, 2000, 3000, and 4000 mL/min through both center pipes. The maximum temperature difference from testing was 0.85°C from water flowing through the center 6' pipe with both ends open at a 4000mL/min flow rate.

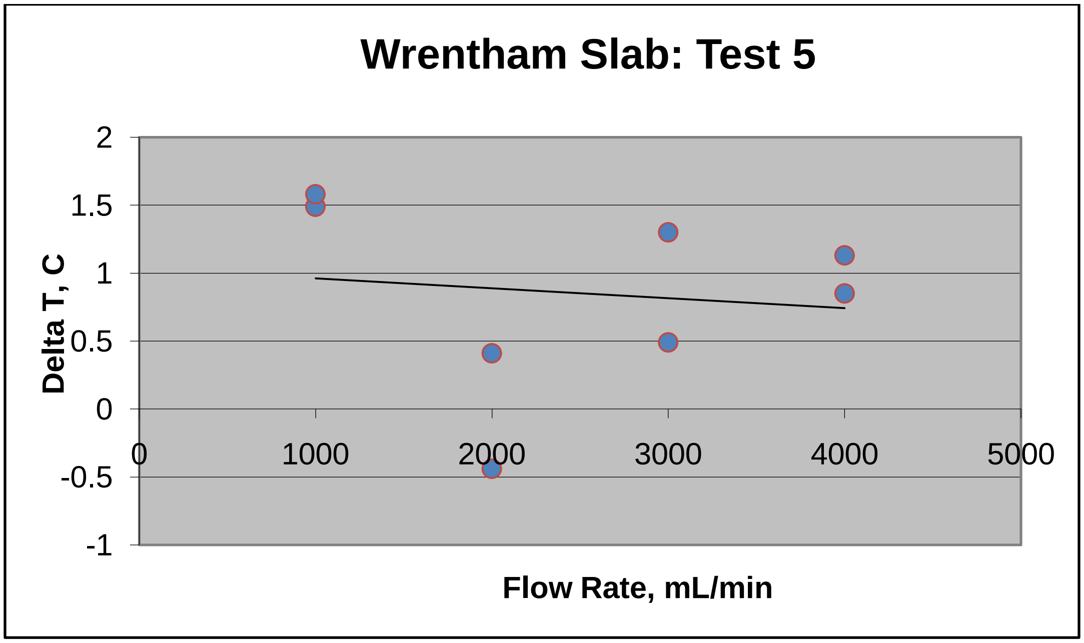

The graph displays no correlation from flow rate to temperature difference. The third data point shows that there was a decrease in temperature difference. This may be the result of thermocouple movement during testing.

Test 6: Quartzite Mix

The 2/3 quartzite and 1/3 granite mix slab when tested at a flow rate of 1000, 2000, 3000, and 4000 mL/min at both center pipes resulted in a maximum temperature difference of 2.17°C at a flow rate of 100mL/min. The lower flow rates produced the greater results in temperature increase.

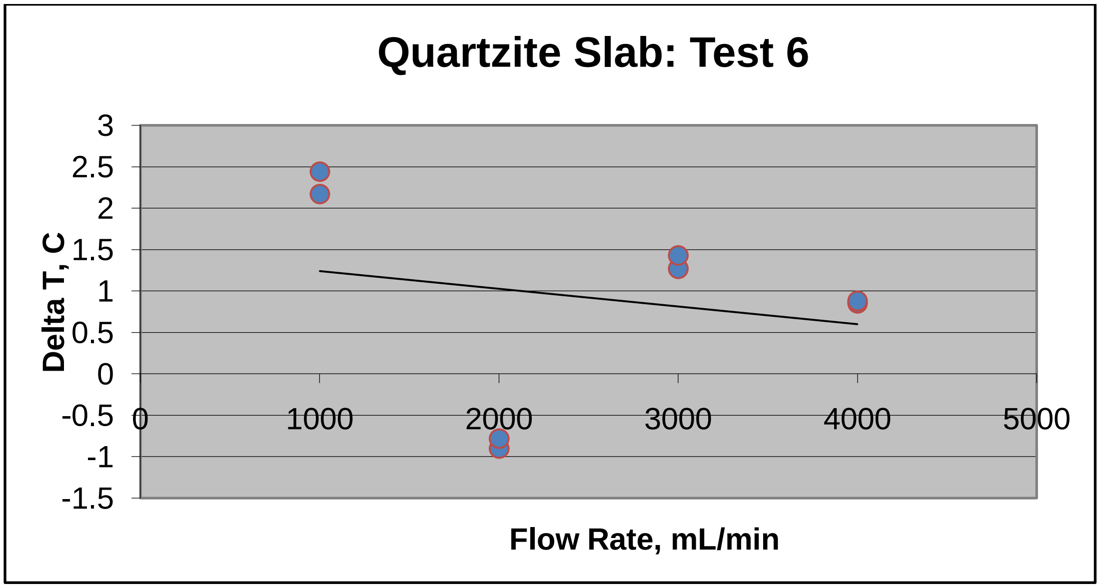

Figure 55: Quartzite Slab - Test 6

Figure 56: Quartzite Slab - Test 6

The temperature difference in the graph of Test 6 shows that as flow rate increase, the difference in temperature decreases. The 3rd and 4th data points display a decrease in temperature. This is suspected to be the result of difficulty with thermocouple setups on the surface of the sample.

Test 7: Wrentham Mix w/ Acrylic Paint Topcoat

The granite slab was tested with 1/3 acrylic paint on surface at a steady state without any water flow and produced the following resulted in minimal difference from the control slab to the acrylic paint.

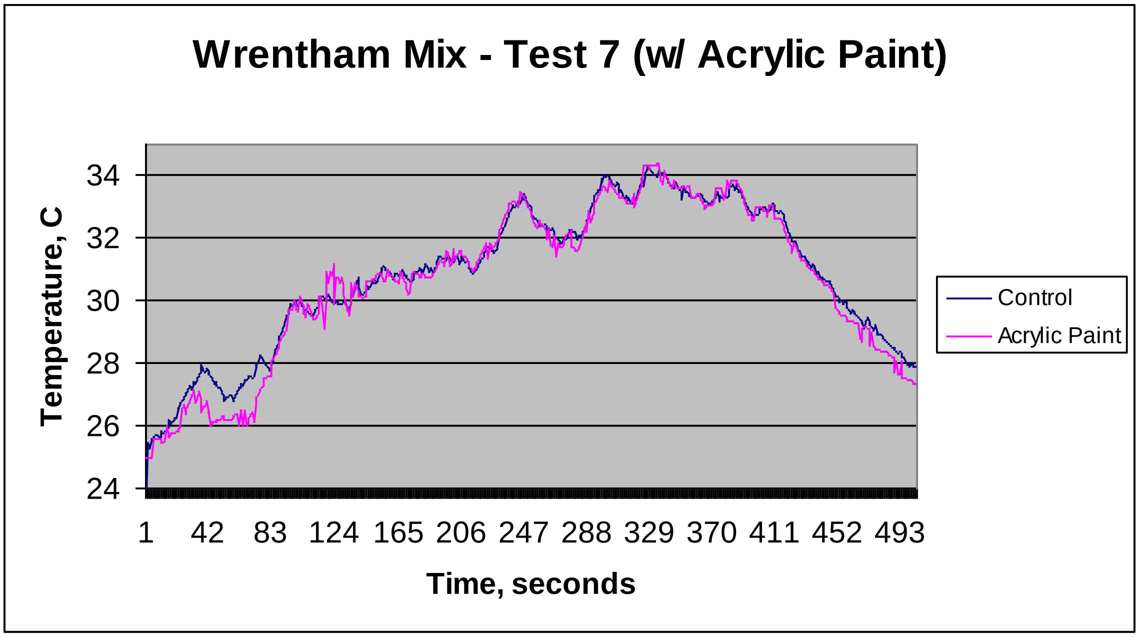

Figure 57: Wrentham Mix - Test 7

The graph showing only the thermocouple placed 1" below the surface for a control slab (the half of the slab not covered with a topcoat) and the granite slab with an acrylic paint topcoat display insignificant differences in temperature increases without any water flow.

Test 8: Quartzite Mix

The 2/3 quartzite and 1/3 granite mix slab test was also tested with flow rate of 1000, 2000, 3000, 4000mL at right end pipe and 1000mL/min at right and center pipes. The maximum heat difference was 6.97 and was achieved at a flow rate of 100mL/min.

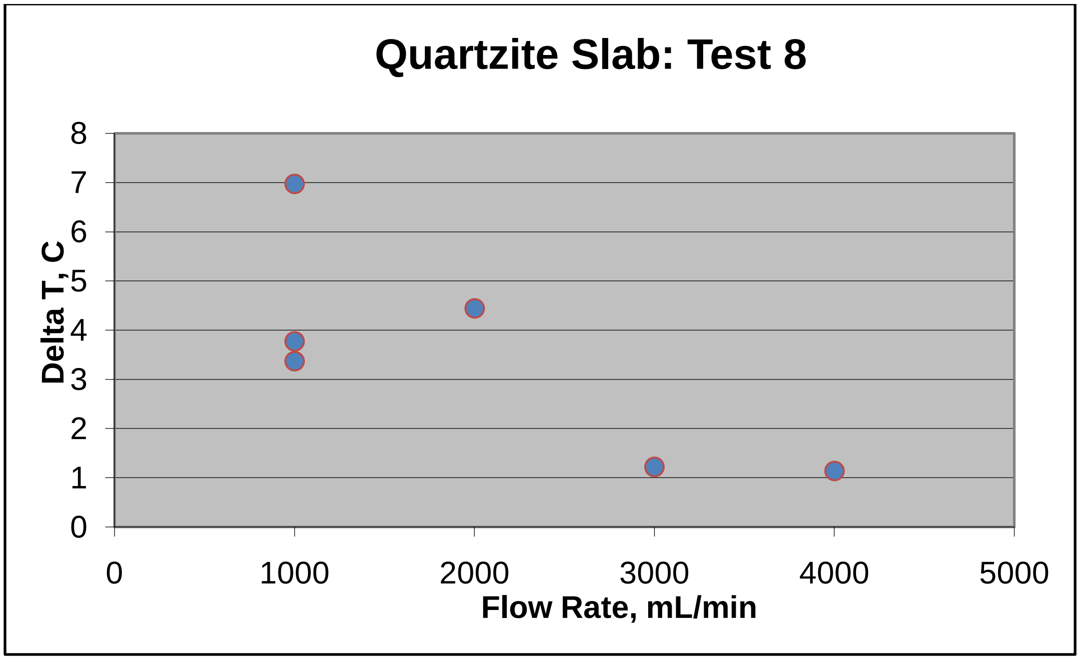

Figure 58: Quartzite Slab - Test 8

The graph of Test 7 for the quartzite slab clearly displays that as flow rate increase, the temperature difference will decrease.

Conclusions and Recommendations

The following conclusions and recommendations can be made from this study.

- Quartzite is more thermally conductive than granite. It has a higher thermal capacity and therefore would be more beneficial to use than granite.
- Flowing water though copper pipes in a heated asphalt pavement sample produces more energy than heating water bath outside of the sample.
- The standing water test concluded that the final water temperature will not increase past a certain point no matter the duration of time the water sits in the pipe.
- Placing glass or Plexiglas on top of the sample makes no significant difference in the temperature increase produced by the pavement compared to an unaltered sample.
- A larger surface area of pavement creates higher temperature difference which result in the production of more energy and therefore more power.
- A proportionally larger surface area of the enclosed pipe produces more energy. The pipe size should be decided based on the size of the pavement.
    - Greater temperature differences are produced from a lower flow rates.
- Using a copper powder additive to the pavement mixture made slight improvement when compared to an unaltered pavement sample, but would not be a sensible additive due to how minor the increases were.
- Acrylic paint only slight improvements to the pavement and would not be recommended as a topcoat for future projects.
- Testing procedures may be improved by developing better methods of securing thermocouples to surface of samples.

From this project, it is recommended that quartzite be used to construct the asphalt pavement parking lots with at least ¾" copper pipes constructed in a system below the compacted pavement. By pumping water though the system at approximately 10mL/min will optimize the energy production. The sample size should be taken into consideration when determining optimum flow rates. As of the conclusion of this project, there were no additives found that would increase the thermal conductivity or capacity to a great enough degree that it would be beneficial to use for the construction of these asphalt pavements.

References

1. Nave, Carl R; Hyperphysics hosted by the Department of Physics and Astrology, Georgia Tech University; (©2005)
   Retrieved November 17, 2007
   http://hyperphysics.phy-astr.gsu.edu/hbase/thermo/heatranex.html#c1
2. .National Cooperative Highway Research Program (NCHRP). "Guide for Mechanistic-Empirical Design." Transportation Research Board, Washington, DC, Design Inputs, March 2004.
3. National Renewable Energy Laboratory (NREL); (November 20, 2006)
   Retrieved November 12, 2007
   http://www.nrel.gov/learning/re_geothermal.html
4. Energy Information Administration (EIA), Energy Kid's Page, (July 2007)
   Retrieved December 4, 2007
   http://www.eia.doe.gov/kids/energyfacts/sources/renewable/geothermal.html
5. Invisible Heating Systems; Road Energy Systems
   Retrieved September 4, 2007
   http://www.invisibleheating.co.uk/road-energy-system-g.asp
6. Huang, Cao, Chen, Shu, He (2006); Laboratory Investigation into Electrically Conductive HMA Mixtures. 2006 Journal of the Association of Asphalt Paving Technologists; *Vol. 75*
7. Marble Institute of America, R-Value of Natural Stone (2007)
   Retrieved October 5, 2007
   http://www.marble-institute.com/industryresources/rvalue.cfm

Appendices

Equations for Results

Using the following equations, power and energy for each of the experiments was calculated.

$$\boldsymbol{Energy = c \times m \times \Delta T}$$

c is the specific heat of water
m is the mass of water
ΔT is the difference in temperature of the water tested

$$\boldsymbol{Power = \frac{Energy}{Time}}$$

Small Sample Results

Case	Diameter of Copper tube	Rate of flow, R, ml/min	Time, t, mins	Time, t, sec.	Volume of flow, V, ml	Change in temperature, delta T, C	Mass, g	Heat, Q, Joules
1	1/2"	not applicable		21600.	not applicable	10.13	570.00	24176.16
2	1/2"	not applicable		21600.	not applicable	5.02	570.00	11980.68
3	1/2"	not applicable		21600.	not applicable	10.47	570.00	24987.60
4	1/2"	3	5.00	300.00	15.00	36.03	15.00	2262.86
		3	10.00	600.00	30.00	28.93	30.00	3633.90
		3	15.00	900.00	45.00	31.92	45.00	6014.21
		3	20.00	1200.0	60.00	29.16	60.00	7325.58
		3	30.00	1800.0	90.00	27.32	90.00	10295.00
5	1/4"	1	119	7140.0	119	3.58	119.00	1783.75
		5	91	5460.0	455	11.99	455.00	22841.97
		8	50	3000.0	400	12.05	400.00	20181.34
		10	60	3600.0	600	9.06	600.00	22760.53
		20	60	3600.0	1200	5.75	1200.00	28890.30
		30	40	2400.0	1200	4.16	1200.00	20901.50
		40	30	1800.0	1200	3.28	1200.00	16480.03
		50	20	1200.0	1000	2.89	1000.00	12100.43
		60	20	1200.0	1200	2.14	1200.00	10752.22
		70	20	1200.0	1400	2.08	1400.00	12192.54
		80	20	1200.0	1600	1.87	1600.00	12527.50
		90	20	1200.0	1800	1.87	1800.00	14093.44
		100	12	720.00	1200	1.98	1200.00	9948.31
6	3/4"	10	116	6960.0	1160.00	36.7	1160.00	178248.9
		20	104	6240.0	2080.00	30.6	2080.00	266494.2
		30	46	2760.0	1380.00	23.4	1380.00	135206.6
		40	54	3240.0	2160.00	19.8	2160.00	179069.6
		60	56	3360.0	3360.00	15.1	3360.00	212431.6
		80	81	4860.0	6480.00	12.4	6480.00	336433.8
		100	61	3660.0	6100.00	12.3	6100.00	314150.6
7	1/4"	1	115	6900.0	115.00	8.08	115.00	3890.56
		5	121	7260.0	605.00	10.35	605.00	26217.95
		8	96	5760.0	768.00	7.68	768.00	24695.93
		10	104	6240.0	1040.00	6.96	1040.00	30307.18
		20	58	3480.0	1160.00	4.15	1160.00	20156.22
		30	44	2640.0	1320.00	2.90	1320.00	16027.84
		40	30	1800.0	1200.00	2.34	1200.00	11757.10

		50	36	2160.0	1800.00	2.09	1800.00	15751.49
		60	22	1320.0	1320.00	1.85	1320.00	10224.65
		70	14	840.0	980.00	1.69	980.00	6934.51
		80	20	1200.0	1600.00	1.67	1600.00	11187.66
		90	26	1560.0	2340.00	1.71	2340.00	16753.86
		100	24	1440.0	2400.00	1.66	2400.00	16681.01
8	1/4"	1	100	6000.0	100.00	10.94	100.00	4580.58
		5	91	5460.0	455.00	11.39	455.00	21698.92
		8	80	4800.0	640.00	9.40	640.00	25188.99
		10	114	6840.0	1140.00	7.51	1140.00	35846.58
		20	77	4620.0	1540.00	4.23	1540.00	27274.96
		30	34	2040.0	1020.00	2.94	1020.00	12555.98
		40	41	2460.0	1640.00	2.32	1640.00	15930.70
		50	38	2280.0	1900.00	1.95	1900.00	15512.84
		60	26	1560.0	1560.00	1.84	1560.00	12018.36
		70	25	1500.0	1750.00	1.74	1750.00	12749.42
		80	22	1320.0	1760.00	1.63	1760.00	12011.67
		90	21	1260.0	1890.00	1.62	1890.00	12819.76
		100	30	1800.0	3000.00	1.70	3000.00	21353.70
9	1/4"	1	83	4980.0	83.00	11.48	83.00	3989.54
		5	123	7380.0	615.00	11.50	615.00	29612.56
		8	121	7260.0	968.00	9.46	968.00	38341.53
		10	112	6720.0	1120.00	8.27	1120.00	38781.67
		20	65	3900.0	1300.00	5.01	1300.00	27269.93
		30	45	2700.0	1350.00	3.87	1350.00	21874.98
		40	44	2640.0	1760.00	3.18	1760.00	23433.80
		50	33	1980.0	1650.00	2.94	1650.00	20311.14
		60	25	1500.0	1500.00	2.77	1500.00	17396.99
		70	21	1260.0	1470.00	2.60	1470.00	16002.71
		80	22	1320.0	1760.00	2.49	1760.00	18349.11
		90	32	1920.0	2880.00	2.38	2880.00	28699.37
		100	24	1440.0	2400.00	2.28	2400.00	22911.26
10	1/4"	1	106	6360.0	106.00	8.28	106.00	3674.85
		5	130	7800.0	650.00	9.66	650.00	26290.17
		8	78	4680.0	624.00	8.17	624.00	21345.66
		10	75	4500.0	750.00	6.56	750.00	20600.04
		20	42	2520.0	840.00	4.35	840.00	15299.30
		30	42	2520.0	1260.00	3.47	1260.00	18306.40
		40	33	1980.0	1320.00	2.90	1320.00	16027.84
		50	32	1920.0	1600.00	2.64	1600.00	17685.89
		60	38	2280.0	2280.00	2.53	2280.00	24152.29
		70	24	1440.0	1680.00	2.34	1680.00	16459.93
		80	23	1380.0	1840.00	2.32	1840.00	17873.47
		90	20	1200.0	1800.00	2.27	1800.00	17108.08
		100	21	1260.0	2100.00	2.32	2100.00	20399.06

11	1/4"	1	70	4200.0	70.00	9.04	70.00	2649.53
		5	64	3840.0	320.00	11.76	320.00	15756.52
		8	95	5700.0	760.00	10.61	760.00	33762.29
		10	89	5340.0	890.00	8.13	890.00	30295.88
		20	57	3420.0	1140.00	4.96	1140.00	23674.97
		30	25	1500.0	750.00	3.47	750.00	10896.67
		40	33	1980.0	1320.00	2.95	1320.00	16304.18
		50	32	1920.0	1600.00	2.52	1600.00	16881.98
		60	29	1740.0	1740.00	2.31	1740.00	16829.23
		70	58	3480.0	4060.00	2.11	4060.00	35868.35
		80	33	1980.0	2640.00	2.00	2640.00	22107.36
		90	24	1440.0	2160.00	1.92	2160.00	17364.33
		100	27	1620.0	2700.00	1.91	2700.00	21592.36
12	1/4"	1	56	3360.0	56.00	6.20	56.00	1453.73
		5	67	4020.0	335.00	10.02	335.00	14054.50
		10	66	3960.0	660.00	7.03	660.00	19426.84
		20	34	2040.0	680.00	4.44	680.00	12641.39
		40	23	1380.0	920.00	2.91	920.00	11209.44
		60	15	900.00	900.00	2.42	900.00	9119.29
		80	18	1080.0	1440.00	2.09	1440.00	12601.20
		100	16	960.00	1600.00	2.12	1600.00	14202.30
13	1/4”	1	107	6420	107.00	5.21	107.00	2334.13
		5	77	4620	385.00	8.77	385.00	14137.20
		10	65	3900	650.00	6.09	650.00	16574.24
		20	38	2280	760.00	3.58	760.00	11391.99
		40	28	1680	1120.00	1.65	1120.00	7737.58
		60	22	1320	1320.00	1.09	1320.00	6024.26
		80	22	1320	1760.00	0.89	1760.00	6558.52
		100	21	1260	2100.00	0.74	2100.00	6506.60
14	1/4"	1	89.00	5340	89.00	11.07	89.00	2254.49
		5	68.00	4080	340.00	8.52	340.00	15759.03
		10	79.00	4740	790.00	4.74	790.00	28181.86
		20	24.00	1440	480.00	2.53	480.00	9526.26
		40	22.00	1320	880.00	1.89	880.00	9321.94
		60	18.00	1080	1080.00	1.7	1080.00	8546.50
		80	16.00	960	1280.00	1.54	1280.00	9110.91
		100	14.00	840	1400.00	11.07	1400.00	9027.17
15	1/4”	5	75.00	4500	375.00	12.82	375.00	20129.00
		10	54.00	3240	540.00	8.4	540.00	18992.23
		20	52.00	3120	1040.00	4.18	1040.00	18201.73
		40	47.00	2820	1880.00	2.16	1880.00	17002.57
		60	56.00	3360	3360.00	1.57	3360.00	22087.26
		80	19.00	1140	1520.00	1.09	1520.00	6937.02

d

		100	19.00	1140	1900.00	1.06	1900.00	8432.62
16	1/4”	5	65.00	3900	325.00	11.02	325.00	14995.74
		10	62.00	3720	620.00	7.05	620.00	18301.38
		20	30.00	1800	600.00	3.17	600.00	7963.67
		40	39.00	2340	1560.00	1.06	1560.00	6923.62
		60	46.00	2760	2760.00	0.32	2760.00	3697.96
		80	33.00	1980	2640.00	-0.06	2640.00	-663.22
		100	14.00	840	1400.00	-0.19	1400.00	-1113.74
17	1/4"	5	74.00	4440	370.00	8.5	370.00	13168.12
		10	64.00	3840	640.00	6.9	640.00	18489.79
		20	52.00	3120	1040.00	3.7	1040.00	16111.58
		40	45.00	2700	1800.00	1.2	1800.00	9043.92
		60	51.00	3060	3060.00	0.8	3060.00	10249.78
		80	31.00	1860	2480.00	0.7	2480.00	7268.63
		100	28.00	1680	2800.00	0.7	2800.00	8206.52

Slab Results

Case	Diameter of Copper tube	Rate of flow, R, mL/min	Volume of flow, V, ml	Δ T, °C	Mass, g	Heat, Q, Joules
1	3/4"	N/A	N/A	N/A	N/A	N/A
2	3/4"	N/A	N/A	N/A	N/A	N/A
3	3/4" (3 ft end open)	300	9300	6.33	300	7951.113
	3/4" (3 ft end open)	1000	29000	4.85	1000	20306.95
	3/4" (6 ft end open)	300	10200	7.18	300	9018.798
	3/4" (6 ft end open)	1000	24000	5.04	1000	21102.48
	3/4" (3 ft)(both open)	500	16500	5.43	500	11367.705
	3/4" (6 ft)(both open)	500	16500	6.67	500	13963.645
	3/4" (3 ft)(both open)	1000	29000	2.58	1000	10802.46
	3/4" (6 ft)(both open)	1000	29000	3.19	1000	13356.53
4	3/4" (3 ft end open)	300	9600	5.33	300	6695.013
	3/4" (3 ft end open)	1000	28000	4.67	1000	19553.29
	3/4" (6 ft end open)	300	10500	8.18	300	10274.898
	3/4" (6 ft end open)	1000	28000	9.33	1000	39064.71
	3/4" (3 ft)(both open)	500	16500	5.77	500	12079.495
	3/4" (6 ft)(both open)	500	16500	7.25	500	15177.875
	3/4" (3 ft)(both open)	1000	28000	3.31	1000	13858.97
	3/4" (6 ft)(both open)	1000	28000	3.93	1000	16454.91
5	3/4" (3 ft)(both open)	1000	29000	1.49	1000	6238.63
	3/4" (6 ft)(both open)	1000	29000	1.58	1000	6615.46
	3/4" (3 ft)(both open)	2000	60000	-0.44	2000	-3684.56
	3/4" (6 ft)(both open)	2000	60000	0.41	2000	3433.34
	3/4" (3 ft)(both open)	3000	90000	0.49	3000	6154.89
	3/4" (6 ft)(both open)	3000	90000	1.3	3000	16329.3
	3/4" (3 ft)(both open)	4000	280000	0.85	4000	14235.8
	3/4" (6 ft)(both open)	4000	280000	1.13	4000	18925.24
6	3/4" (3 ft)(both open)	1000	30000	2.17	1000	9085.79
	3/4" (6 ft)(both open)	1000	30000	2.44	1000	10216.28
	3/4" (3 ft)(both open)	2000	60000	-0.9	2000	-7536.6
	3/4" (6 ft)(both open)	2000	60000	-0.78	2000	-6531.72
	3/4" (3 ft)(both open)	3000	90000	1.27	3000	15952.47
	3/4" (6 ft)(both open)	3000	90000	1.43	3000	17962.23
	3/4" (3 ft)(both open)	4000	280000	0.85	4000	14235.8
	3/4" (6 ft)(both open)	4000	280000	0.88	4000	14738.24
7	3/4"	N/A	N/A	N/A	N/A	N/A
8	3/4" (3 ft)(right end open)	1000	35000	6.97	1000	29183.39
	3/4" (3 ft)(right end open)	2000	70000	4.44	2000	37180.56
	3/4" (3 ft)(right end open)	3000	108000	1.22	3000	15324.42
	3/4" (3 ft)(right end open)	4000	112000	1.14	4000	19092.72
	3/4" (3 ft)(right end open)	1000	38000	3.37	1000	14110.19
	3/4" (3 ft)(center end open)	1000	38000	3.77	1000	15784.99

Gradation for Quartzite Aggregates

The following table shows the gradation for the Sioux quartzite aggregates used in the mix design.

Sieve size, mm	***% Passing Target***
19.00	100.0
12.50	96.2
9.50	82.0
4.75	67.5
2.36	53.0
1.18	37.0
0.60	25.2
0.30	12.9
0.150	6.3
0.075	3.1